Section 2 Plasma Physics

Chapter 1. Plasma Dynamics

Academic and Research Staff

Professor George Bekefi,[1] Professor Abraham Bers, Professor Bruno Coppi, Professor Jonathan S. Wurtele, Dr. Chiping Chen, Dr. Stefano Migliuolo, Dr. Abhay K. Ram, Dr. Richard Stoner,[2] Dr. Linda E. Sugiyama, Ivan Mastovsky

Visiting Scientists and Research Affiliates

Dr. Augusta Airoldi, Dr. Giuseppe Bertin, Dr. Francesca Bombarda, Franco Carpignano, Dr. Giovanna Cenacchi, Dr. Paolo Detragiache, Dr. Matteo Erba, Dr. Vladimir Fuchs,[3] Dr. Riccardo Maggiora, Dr. Francesco Pegoraro, Marco Riccitelli, Dr. Suraj Salihu, George M. Svolos, Dr. Motohiko Tanaka, Dr. Joachim Theilhaber,[4] Dr. Ian Wilson,[5] Dr. Walter Wuensch[5]

Graduate Students

Palmyra E. Catravas, William S. Daughton, Darin R. Ernst, Felicisimo W. Galicia, Steven D. Schultz, Gregory E. Penn, Darren M. Pierre, Caterina Riconda, Luigi Vacca

Undergraduate Students

Gianmarco M. Felice, MöH Kuang, Kevin Lewis, Evan Reich, Jeremy Roy

Technical and Support Staff

Felicia G. Brady, Marika Contos, Laura von Bosau, Miriam Weiner

1.1 MIT Microwiggler for Free Electron Laser Applications

Sponsor

U.S. Navy - Office of Naval Research
Grant N00014-90-J-4130

Project Staff

Professor George Bekefi, Professor Hermann A. Haus, Professor Jonathan S. Wurtele, Dr. Richard Stoner, Ivan Mastovsky, Palmyra E. Catravas, Marcus Babzien,[6] Ken Batchelor,[6] Dr. Ilan Ben-Zvi,[6] Jimmy Fang,[6] Dr. Alan Fisher,[6] Dr. William Graves,[6] Dr. Zvi Segalov,[6] Joe Qiu,[6] Dr. Xi-Jie Wang[6]

A microwiggler-based FEL permits operation at shorter wavelengths with a reduction in the size and cost of the device. Reduction in the period of the wiggler from the typical 3-10 cm to below 1 cm permits operation of FELs at shorter wavelengths for a given beam energy. The MIT microwiggler is a pulsed ferromagnetic-core electromagnet with 70 periods of 8.8 mm each which generates an on-axis peak magnetic field of 4.2 kG. The pulse repetition rate is 0.5 Hz with FWHM 0.5 msec. The microwiggler is characterized by extensive tunability. We employed a novel tuning regimen through which the rms spread in peak amplitudes was reduced to 0.08 percent, the lowest ever achieved in a sub-cm period magnetic field. The microwiggler is a serviceable scientific apparatus. Spontaneous emission has been observed for wavelengths of 500-800 nm using a 40-50 MeV

---

1 Deceased August 17, 1995.

2 Smithsonian Astrophysical Observatory, Cambridge, Massachusetts.

3 Centre Canadien de Fusion Magnétique (CCFM), Québec, Canada.

4 IBM Corporation, Waltham, Massachusetts.

5 CERN, SL-RFL, CH-1211, Geneva 23, Switzerland.

6 Accelerator Test Facility, Brookhaven National Laboratory, Long Island, New York.

beam from the Accelerator Test Facility LINAC at BNL.

High field precision in short-period wigglers is difficult to achieve. Mechanical tolerances and other coil-to-coil variations become sufficiently large on the scale of the wiggler period that they translate easily into field errors of harmful amplitude. The severity of the problem compounds with wiggler length, and curtails the FEL efficiency through deleterious increases in electron beam walk-off and energy spread. Various microwiggler designs have been investigated to address these technical challenges.[7] (see table 1) We have employed a novel approach to reducing wiggler field errors in which extensive tunability is controlled through a rigorous tuning procedure. The high performance of the microwiggler makes it well-suited for the development of a linac-based FEL in the visible and UV wavelengths.

GROUP	TECHNOLOGY AND STATUS	N_w	λ_w,mm / G,mm	B_w, kG	PEAK RMS ERROR	POLE INT. ERROR
Stoner *et al.*, MIT	Pulsed ferrocore electromagnet	70	8.8/ 4.2	4.2	0.08%	0.14%
Huang *et al.*, Stanford	Staggered ferrocore array in solenoid	50	10.0/ 2.0	10.8	1.2%	Not reported
Warren and Fortgang LANL	Permanent magnet	73	13.6/ 1.5	6.5	0.3%	Not reported
Tecimer and Elias CREOL	Hybrid	62	8/ Not reported	1.0	0.2%	0.6%
Ben-Zvi *et al.*, BNL	Superconducting ferrocore electromagnet	68	8.8/ 4.4	>5.5	*	*

* Phase shake and walk-off (+/- 22 μm) reported in lieu of peak amplitude and pole integral spread.

Table 1. Comparison of some short period wigglers.

---

[7] I. Kimel and R. Elias, "Micro-undulator Fields," *Nucl. Instr. and Meth. A* 296: 611-618 (1990); G. Ramian, L. Elias, and I. Kimel, "Micro-undulator FELs," *Nucl. Instr. and Meth. A* 250: 125-133 (1986); J.H. Booske, W.W. Destler, Z. Segalov, D.J. Radack, E.T. Rosenbury, J. Rodgers, T.M. Antonsen, Jr., V.L. Granatstein, and I.D. Mayergoyz, "Propagation of Wiggler Focused Relativistic Sheet Electron Beams," *J. Appl. Phys.* 64: 6-11 (1988); V.A. Papadichev and O.A. Smith, "Helical Microundulators of the P.N. Lebedev Physical Institute," *Nucl. Instr. and Meth. A* 318: 803-808 (1992); R.W. Warren, D.W. Feldman, and D. Preston, "High-Field Pulsed Microwigglers," *Nucl. Instr. and Meth. A* 296: 558-562 (1990); C.M. Fortgang and R.W. Warren, "Measurement and Correction of Magnetic Fields in Pulsed Slotted-tube Microwigglers," *Nucl. Instr. and Meth. A* 341: 436-439 (1994); R.W. Warren and C.M. Fortgang, "Fabrication of High-Field Short-period Permanent Magnet Wigglers," *Nucl. Instr. and Meth. A* 341: 444-448 (1994); Y.C. Huang, H.C. Wang, R.H. Pantell, J. Feinstein, and J. W. Lewellen, "A Staggered-Array Wiggler for Far-Infrared, Free-Electron Laser Operation," *IEEE J. Quant. Electron.* 30(5): 1289-1294 (1994). N. Ohigashi, K. Mima, Y. Tsunawaki, S. Ishii, N. Ikeda, K. Imasaki, M. Fujita, S. Kuruma, A. Murai, C. Yamanaka, and S. Nakai, "Development of an Electromagnetic Helical Microwiggler," *Nucl. Inst. and Meth. A* 341: 426-430 (1994); I. Ben-Zvi, R. Fernow, J. Gallardo, G. Ingold, W. Sampson and M. Woodle, "Performance of a Superconducting, High Field Subcentimeter Undulator," *Nucl. Instr. and Meth. A* 318: 781-788 (1992); G. Ingold, I. Ben-Zvi, L. Solomon, and M. Woodle, "Fabrication of a High-Field Short-period Superconducting Undulator," submitted to *Proceedings of the 17th International Free Electron Laser Conference,* New York, 1995; M. Tecimer and L.R. Elias, "Hybrid Microundulator Designs for the CREOL Compact cw-FEL," *Nucl. Instr. and Meth. A* 341: ABS126-ABS127 (1994); R. Stoner, S.-C. Chen, and G. Bekefi, "A Planar Electromagnet Microwiggler for Free Electron Lasers," *IEEE Trans. Plasma Sci.* 18: 387-391 (1990).

PARAMETER	VALUE
on-axis magnetic field, B_w	4.2 kG
wiggler period, λ_w	8.8 mm
wiggler parameter, a_w	0.34
wiggler gap, G	4.2 mm
number of periods, N_w	70
rms spread in peak amplitudes, $(\delta B/B)_{RMS}$	0.08%
rms spread in pole integrals, $(\delta I/I)_{RMS}$	0.14%
repetition rate	0.5 Hz

Table 2. MIT Microwiggler parameters.

1.1.1 Microwiggler Field Characteristics

Table 2 summarizes the microwiggler parameters. Wiggler design, construction and tuning algorithm are detailed in Stoner and Bekefi.[8] The measurements of field characteristics described here are for the full 70 periods (excluding tapered end effects) and for a repetition rate of 0.5 Hz. Each half period in the wiggler is created by a pair of magnets connected electrically in parallel, which are mounted on either side of a stainless steel bore in a precisely formed aluminum matrix (see figure 1). Current flows independently to each pair of magnets and is controlled by an variable series resistance. In order to completely characterize the microwiggler field characteristics, a comprehensive battery of field measurements was performed.

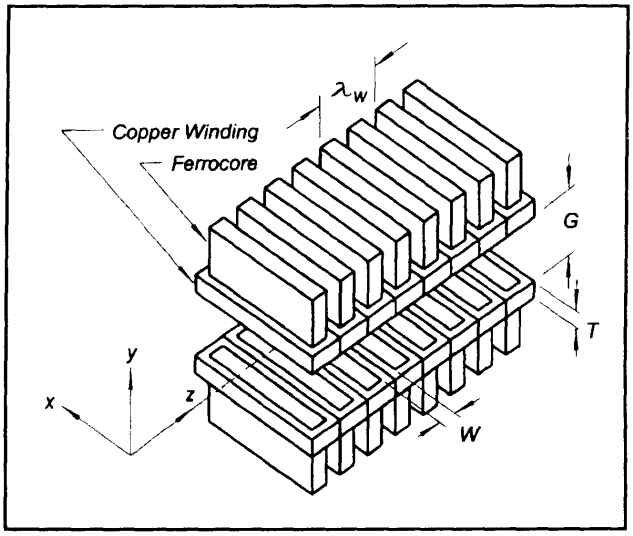

Figure 1. Schematic of the wiggler geometry.

The Measurement System

An automated control system monitors the field profile, in which a B-dot loop is pulled through the bore and recorded. Peak amplitudes and peak axial positions are extracted from curve fits to the data. The control system includes feedback to maintain the wiggler total current at a constant level. Complete field scans are repeated from 5-15 times and averaged, so that a single field profile contains the information of over 10,000 field amplitude data points.

The untuned field profile was dominated by the effects of small inhomogeneities in the wiggler construction and had an rms spread of 4 percent (figure 2). From a consecutive sequence of field profile measurements, tuning iterations reduced the spread in peak amplitudes to 0.08 percent or better, an improvement of nearly two orders of magnitude. This is an outstanding level of uniformity for a sub-cm period wiggler and illustrates the power of our tuning algorithm in controlling the field.

[8] R. Stoner and G. Bekefi, "A 70-Period High-Precision Microwiggler for Free Electron Lasers," *IEEE J. Quant. Electron.* 31: 1158-1165 (1995).

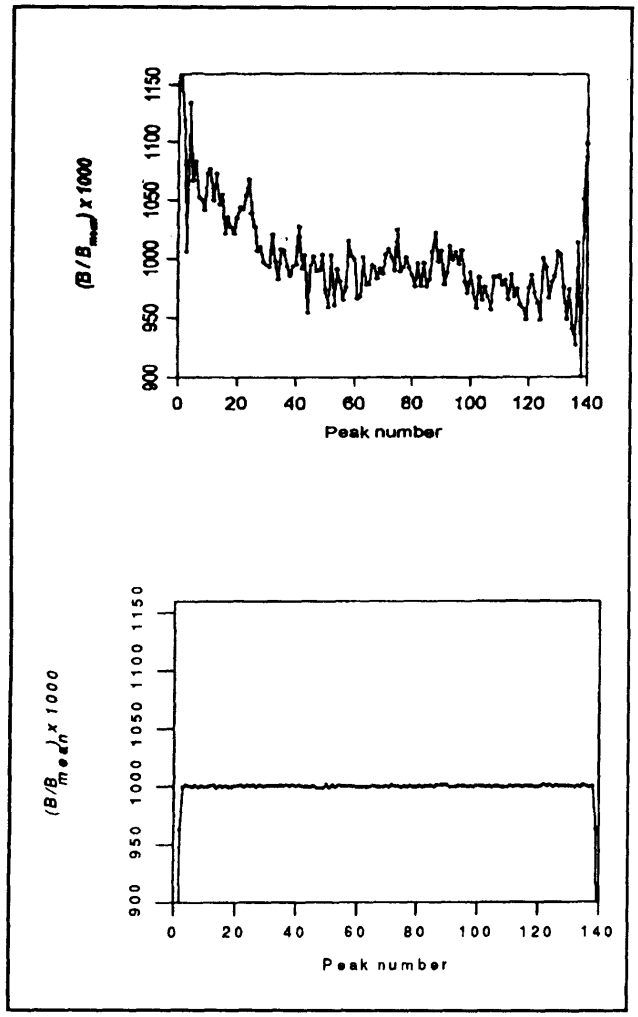

Figure 2. Peak amplitude profile: untuned profile (rms spread 4 percent) and tuned profile (0.08 percent).

A high level of purity in the wiggler field harmonic spectrum was measured and provides an independent confirmation of the peak amplitude uniformity. Furthermore, it is important that the design of the wiggler gap dimension, which must be small for large field amplitudes, does not result in field harmonics, since the high frequency harmonic emissions can damage optical coatings during lasing. Measurements show that the third harmonic is down by more than five orders of magnitude from the fundamental, the fifth harmonic is just above the noise level, and the other harmonics are not measurable.

1.1.2 Spontaneous Emission Measurements

We have been working in collaboration with researchers at the Accelerator Test Facility at Brookhaven National Laboratory to lase at 532 nm with the MIT Microwiggler in a linac-based FEL. Work in the past year has included the setup of a 3.67 m cavity around the wiggler, and the development of system alignment techniques.

Systematic measurements of spontaneous emission as a function of beam parameters are underway, to investiage how the emissions reflect the characteristics of the machine. Appropriate dependence of emissions with electron beam energy (figure 3), energy spread, emittance, and wiggler field strength have been observed. The potential for the wiggler emissions to provide information on beam alignment has been experimentally demonstrated. Single-shot spectra for 20 micropulses and even as low as a single micropulse have been recorded using a CCD camera on the output of the spectrometer. Ringdown of the spontaneous emission in the cavity has been recorded, as well as spontaneous emission trains during full macropulse operation.

1.1.3 Discussion

The high precision field profile of the MIT Microwiggler will permit the generation of coherent radiation at wavelengths ranging from the visible to ultraviolet. With our typical observations of an rms spread of 0.08 percent in peak amplitudes and 0.14 percent in pole integrals, the MIT Microwiggler currently provides the world's most uniform periodic field for any sub-cm period wiggler and is a unique tool for FEL research.

1.1.4 Publications

Babzien, M., I. Ben-Zvi, P. Catravas, J. Fang, A. Fisher, W. Graves, X.-Z. Qin, Z. Segalov and X.-J. Wang. "Optical Diagnostics for the ATF Microundulator FEL." Submitted to the *Proceedings of the 17th International Free Electron Laser Conference,* New York, 1995.

Catravas, P., R. Stoner, J. Blastos, D. Sisson, I. Mastovsky, G. Bekefi, A. Fisher, and X.-J. Wang. "MIT Microwiggler for Free Electron Laser Applications." Paper presented at the Particle Accelerator Conference, Dallas, Texas, 1995.

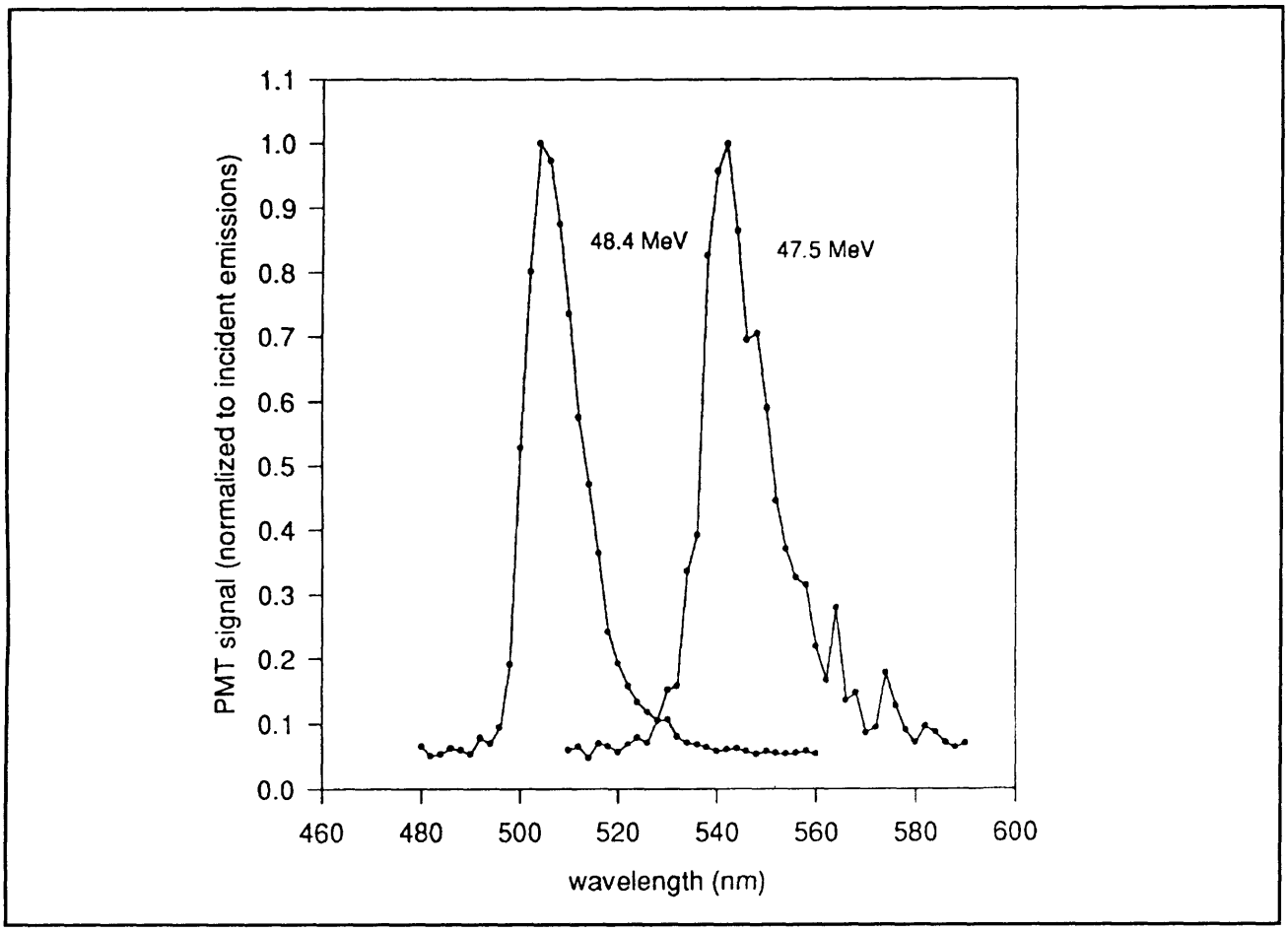

Figure 3. Spontaneous emission spectra for beam energies of 47.5 and 48.4 MeV.

Catravas, P., R. Stoner, and G. Bekefi. "Characteristics of the MIT Microwiggler for Free Electron Laser Applications." Submitted to the *Proceedings of the 17th International Free Electron Laser Conference.* New York, 1995.

Stoner, R., and G. Bekefi. "A 70-Period High-Precision Microwiggler for Free Electron Lasers." *IEEE J. Quantum Electron.* 31(6): 1158-1165 (1995).

1.2 Plasma Wave Interactions—RF Heating and Current Generation

1.2.1 Introduction

The research of this group is concerned with both basic and applied problems in the electrodynamics of plasmas. Attention is directed toward understanding the nonlinear dynamics of plasmas driven by high-frequency electromagnetic fields (such as in laser-plasma interactions or RF heating and current drive of magnetically confined plasmas), the generation and propagation of unstable radiations from anisotropic electron distributions in space and astrophysical plasmas, and the energization of ions to the magnetosphere.

The first two reports describe our progress in the analysis of mode conversion from fast Alfvén waves to ion-Bernstein waves in tokamak confined plasmas. Recent experiments (TFTR at Princeton, Tore Supra in Cadarache, France, and Alcator C-MOD at MIT) have shown that mode-converted ion-Bernstein waves are effective in producing localized electron heating. Very recent experiments on TFTR have also produced localized plasma currents with such waves, and this may prove to be an important means for significantly enhancing the quality and operation of tokamak plasmas. The third report describes our continuing effort at exploring a possible synergism between RF driven currents and the bootstrap current for steady state confinement of tokamak plasmas. The fourth report describes an evaluation of a new transport mechanism of minority ion energy loss in tokamak plasmas intensely heated by ion-cyclotron RF

power. Finally, the last report takes a new look at induced stochasticity in ion dynamics in an electrostatic wave propagating across the magnetic field. This study is aimed at exploring its possible application toward understanding the transverse acceleration of O^+ and H^+ ions from the ionosphere to the magnetosphere where they are observed.

1.2.2 Mode Conversion of Fast Alfvén Waves to Ion-Bernstein Waves

Sponsors

Princeton University/Tokamak Physics Experiment
Grant S-03688-G
U.S. Department of Energy
Grant DE-FG02-91-ER-54109

Project Staff

Dr. Abhay K. Ram, Professor Abraham Bers, Dr. Vladimir Fuchs, Steven D. Schultz

A successful way of delivering radio frequency power for heating a tokamak plasma has been through fast Alfvén waves (FAW), excited by antennas on the low-field side of a tokamak, in the ion-cyclotron range of frequencies (ICRF). In a plasma consisting of at least two ion species with different charge-to-mass ratios, the ion-ion hybrid resonance can be present in the plasma if the frequency of the RF wave is chosen appropriately. In the vicinity of this resonance, the FAW can mode convert to the ion-Bernstein wave (IBW), which then propagates away from the resonance towards the high-field side of the tokamak. In our previous progress report,[9] we described this mode conversion process in the presence of the high-field side, right-hand cutoff of the FAW. We presented a physical model, based on a modified Budden-type analysis that included the right-hand cutoff, which showed that the power mode-conversion coefficient to IBWs could be a maximum of 100 percent. The mode-conversion coefficient depended on the phase difference between the FAW incident on the right-hand cutoff and the FAW reflected from this cutoff. We have since formulated the technique for calculating this phase for more realistic representations of the FAW dispersion relation. This is described below in detail.

In a simple, one-dimensional (equatorial plane) description, the approximate cold-plasma dispersion relation for the FAW is:

$$n_\perp^2 = \frac{(L - n_\parallel^2)(R - n_\parallel^2)}{S - n_\parallel^2} \tag{1}$$

where all the symbols and their significance are described in last year's progress report.[9] The propagation of the FAW through the resonance and the cutoffs is thus described by a differential equation:

$$\frac{d^2E}{d\xi^2} + Q(\xi)E = 0 \tag{2}$$

where E is the poloidal component of the electric field, $\xi = \omega x/c$ is the normalized spatial coordinate along the equatorial plane, and $Q(\xi)$ is the "potential" function, which for a cold plasma is equal to the right-hand side of (1).

For the propagation of FAW incident on the left-hand cutoff ($L = n_\parallel^2$) and propagating through the resonance ($S = n_\parallel^2$) to the high-field side right-hand cutoff ($R = n_\parallel^2$), the model potential in (2) is taken to be given by:

$$Q(\xi) = \begin{cases} \gamma - \dfrac{\beta}{\xi}, & \text{if } \xi > 0 \\ \alpha\xi + \tilde{\gamma} - \dfrac{\beta}{\xi}, & \text{if } \xi \le 0 \end{cases} \tag{3}$$

and α, β, γ, and $\tilde{\gamma}$ are parameters that are determined from a fit to the local fast wave dispersion relation. For $\xi > 0$, (3) gives the usual Budden potential with $\gamma > 0$ and $\beta > 0$. The right-hand cutoff is given by $Q(\xi) = 0$ for $\xi < 0$. We will assume that near the right-hand cutoff $|\beta/\xi|$ is very small compared to $|\alpha\xi|$ and $\tilde{\gamma}$, so that this cutoff is approximately given by $\xi_R = -\tilde{\gamma}/\alpha$. Since for $\xi < \xi_R$ we assume that the solutions to (2) are evanescent, it follows that $\alpha > 0$ and $\tilde{\gamma} > 0$. A model $Q(\xi)$ plotted in figure 4 shows characteristics very similar to those of the FAW dispersion relation between the high-field side cutoff and the left-hand cutoff.

---

[9] A. Bers, A.K. Ram, C.C. Chow, V. Fuchs, K.P. Chan, S.D. Schultz, and L. Vacca, "Plasma Wave Interactions—RF Heating and Current Generation," *RLE Progress Report* 137: 229-237 (1994).

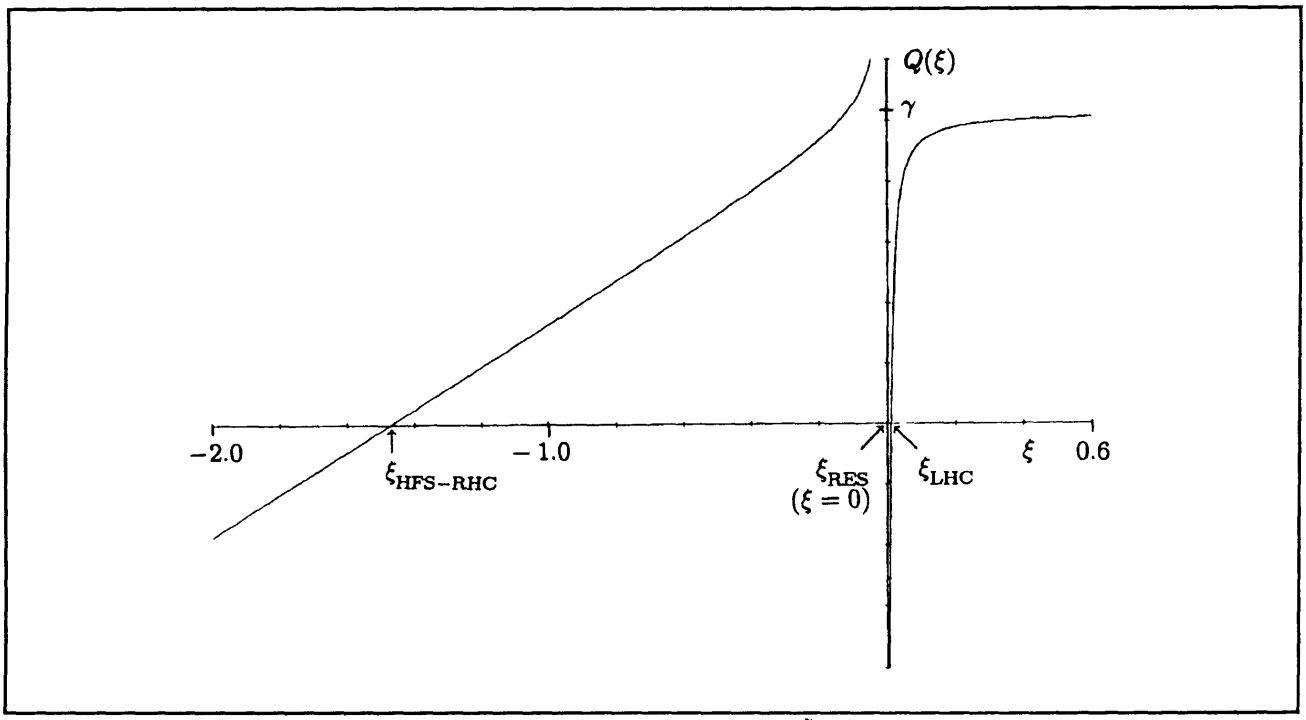

Figure 4. The model potential of equation (3) for $\alpha = 351$, $\beta = 5$, and $\gamma = \tilde{\gamma} = 513.6$. The locations of the high-field side right-hand cutoff, the ion-ion hybrid resonance, and the left-hand cutoff are denoted by $\xi_{HFS-RHC}$, ξ_{RES}, and ξ_{LHC}, respectively.

The solution to (2) and (3) is obtained by determining the solutions for $\xi < 0$ (referred to as Region I) and for $\xi > 0$ (Region II) and matching them across $\xi = 0$. In Region II, the solutions are given by the usual Whittaker functions. In Region I, there does not exist a closed form solution in terms of known functions. However, by subdividing Region I into three subregions and doing uniform asymptotic matching[10] across these three subregions, we obtain an approximate solution in Region I. The matching conditions at $\xi = 0$ are:

$$E_{II}(\xi)\Big|_{\xi \to 0^+} = E_I(\xi)\Big|_{\xi \to 0^-}$$

$$\frac{dE_{II}(\xi)}{d\xi}\Big|_{\xi \to 0^+} = \frac{dE_I(\xi)}{d\xi}\Big|_{\xi \to 0^-} + i\pi\beta E(0) \qquad (4)$$

where 0^+ or 0^- indicates that ξ tends to zero from the positive or the negative side, respectively. The jump condition for the derivative of E can be easily derived since near $\xi = 0$ the potential function is of the form $-\beta/\xi$.

The high-field cutoff ξ_R ensures that the power transmission coefficient is zero. The solution to (2) and (3) will determine the power reflection coefficient R. The mode-conversion coefficient will be C=1 - R. The solution in Region II can be written as:

$$E_{II}(x) = c_{II}W_{\kappa,1/2}(z) + d_{II}W_{-\kappa,1/2}(-z) \qquad (5)$$

where c_{II} and d_{II} are constants determined by the boundary conditions, $W_{\kappa,1/2}(z)$ and $W_{-\kappa,1/2}(-z)$ are the Whittaker functions,[11] and:

$$z = -2i\sqrt{\gamma}\,\xi, \quad \kappa = -\frac{i}{2}\frac{\beta}{\sqrt{\gamma}} \equiv -\frac{i}{2}\eta \qquad (6)$$

[10] C.M. Bender and S.A. Orszag, *Advanced Mathematical Methods for Scientists and Engineers* (New York: McGraw-Hill, 1978).

[11] M. Abramowitz and I.A. Stegun, *Handbook of Mathematical Functions* (New York: Dover Publications, 1970).

Using the asymptotic forms of the Whittaker functions,[12] the power reflection coefficient can be expressed as:

$$R = \left| \frac{c_{II}}{d_{II}} - (1 - e^{\pi\eta})e^{-2i\theta} \right|^2 e^{-2\pi\eta} \qquad (7)$$

where θ is the phase of $\Gamma(-i\eta/2)$. The ratio c_{II}/d_{II} is determined by matching to the solution in Region I. In Region I, as $\xi \rightarrow 0^-$, the solution to (2) and (3) is:

$$\lim_{\xi \rightarrow 0^-} E_I(\xi) = c_I W_{\tilde{\kappa}, 1/2}(\tilde{z}) + d_I W_{-\tilde{\kappa}, 1/2}(-\tilde{z}) \qquad (8)$$

where c_I and d_I are constants, and

$$\tilde{z} = -2i\sqrt{\tilde{\gamma}}\,\xi, \quad \tilde{\kappa} = -\frac{i}{2}\frac{\beta}{\sqrt{\tilde{\gamma}}} = -\frac{i}{2}\tilde{\eta} \qquad (9)$$

From the matching conditions in (4) at $\xi=0$, and using the properties of the Whittaker functions near $\xi=0$,[13] we find:

$$\frac{c_{II}}{d_{II}} = e^{-2i\theta} \frac{\frac{c_I}{d_I} e^{2i\tilde{\theta}} \left\{ A + i\pi + i\pi \coth\left(\frac{\pi\eta}{2}\right) \right\} - \left\{ A + i\pi \coth\left(\frac{\pi\eta}{2}\right) - i\pi \coth\left(\frac{\pi\tilde{\eta}}{2}\right) \right\}}{\frac{c_I}{d_I} e^{2i\tilde{\theta}} A - \left\{ A - i\pi - i\pi \coth\left(\frac{\pi\tilde{\eta}}{2}\right) \right\}} \qquad (10)$$

where

$$A = \frac{1}{2} \ln\left(\frac{\tilde{\gamma}}{\gamma}\right) + \psi_R\left(\frac{i\tilde{\eta}}{2}\right) - \psi_R\left(\frac{i\eta}{2}\right) + i\frac{\pi}{2}\left\{ \coth\left(\frac{\pi\tilde{\eta}}{2}\right) - \coth\left(\frac{\pi\eta}{2}\right) \right\} \qquad (11)$$

$\tilde{\theta}$ is the phase of $\Gamma(-i\tilde{\eta}/2)$, and ψ_R is the real part of the Psi function.[11]

An approximate solution in Region I is obtained by uniform asymptotic matching.[10] We find:

$$\frac{c_I}{d_I} = -i\left(\frac{\alpha}{8i\tilde{\gamma}^{3/2}}\right)^{-i\tilde{\eta}} \exp\left(\frac{\pi\eta}{2}\right) \exp\left(\frac{4i}{3\alpha}\tilde{\gamma}^{3/2}\right) \qquad (12)$$

Since from (12) $|c_I/d_I| = 1$, it can be shown that, from (10), $|c_{II}/d_{II}| = 1$. Thus, we can express $c_{II}/d_{II} = \exp[i(\pi + \phi)]$ where the expression for ϕ can be determined from (10) and (12). Thus, the phase ϕ mentioned in *Progress Report No. 137* is now completely determined for a realistic model of the potential function describing the propagation of FAWs. Substituting (12) into (7) completely determines the reflection coefficient. With this representation, the power mode-conversion coeffecient is:

$$C = 4T_B(1 - T_B)\cos^2\left(\frac{\phi}{2} + \theta\right) \qquad (13)$$

where $T_B = \exp(-\pi\eta)$.

In the special case when $\tilde{\gamma} = \gamma$, we find from (10) and (12) that the phase ϕ is given by:

$$\phi = \frac{4}{3\alpha}\gamma^{3/2} + \eta \ln\left(\frac{8\gamma^{3/2}}{\alpha}\right) + \frac{\pi}{2}$$

$$= \frac{4\sqrt{\gamma}}{3|\xi_R|} + \eta \ln\left(\frac{8\sqrt{\gamma}}{|\xi_R|}\right) + \frac{\pi}{2} \qquad (14)$$

where $\xi_R < 0$ is the location of the right-hand cutoff. Thus, the phase introduced by the right-hand cutoff is related to the distance between the resonance

[12] J. Heading, *J. Math. Soc.* (London) 37: 195 (1962).

[13] H. Buchholz, *The Confluent Hypergeometric Function* (New York: Springer Verlag, 1969).

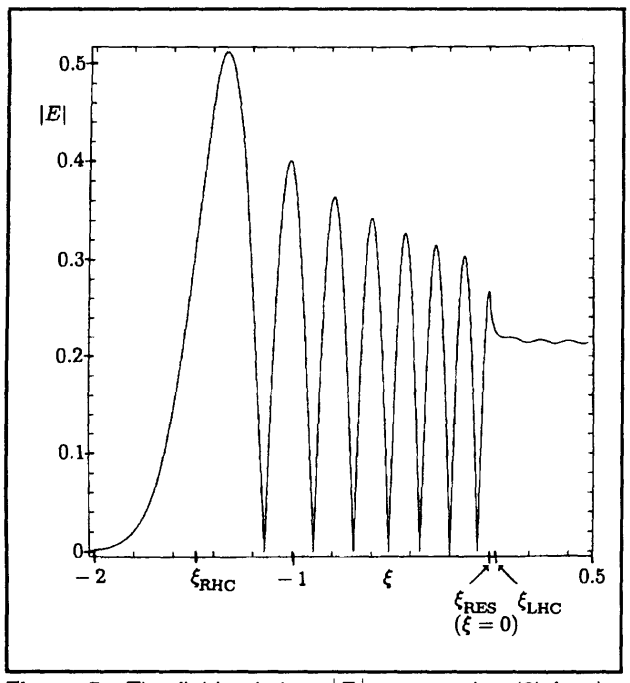

Figure 5. The field solution, $|E|$, to equation (2) for the $Q(\xi)$ given in figure 4. The parameters chosen were such that the reflection coefficient is almost zero and the entire incoming FAW power is mode converted.

and the right-hand cutoff normalized to the FAW wavelength.

The above analysis implies that the triplet system can be viewed as forming an internal plasma resonator which contains resonant absorption. The resonator is intrinsic to the plasma because it does not require a structure external to the plasma—it is formed by features (the cutoffs) that are intrinsic to the plasma. The fast Alfvén wave incident from the low-field side is coupled to the resonator at the left-hand cutoff. This coupling is mainly determined by η which enters into T_B in (13). The resonator is naturally specified by the phases ϕ and θ. However, due to the intrinsically inhomogeneous plasma, these phases are not simply related to some integer multiple of half-wavelengths between the left-hand cutoff and high-field side right-hand cutoff. The dissipation in this resonator occurs at the ion-ion hybrid resonance layer. In the cold plasma model, this is exhibited as resonant absorption; a kinetic description of the ion-ion hybrid resonance layer shows that this is mode conversion of the incident fast Alfvén wave to an ion-Bernstein wave which damps on electrons.[14] The condition for 100 percent mode conversion corresponds to the situation in which the incident fast Alfvén wave is critically coupled to this resonator. Then there is no reflection of the fast Alfvén wave towards the low-field side, and the incident wave power is totally absorbed. Figure 5 shows an example of the internal resonator effect where we have chosen parameters such that $\eta \approx 0.22$. Here there is no reflection, so that the mode-conversion efficiency is nearly 100 percent, and the fields are localized between the resonance and the high-field cutoff.

1.2.3 Mode Conversion to Ion-Bernstein Waves of Fast Alfvén Waves With Finite Poloidal Wavenumber

Sponsors

National Science Foundation
Grant ATM 94-24282
U.S. Department of Energy
Grant DE-FG02-91-ER-54109

Project Staff

Steven D. Schultz, Professor Abraham Bers, Dr. Abhay K. Ram

In *Progress Report No. 137* and in the preceding section, we described ongoing theoretical work on the mode conversion of fast Alfvén waves (FAW) at the ion-ion hybrid resonance. The fraction of power mode converted to ion Bernstein waves was calculated using a resonant absorption model, with the plasma shape near the ion-ion hybrid resonance approximated as a slab which has a uniform magnetic field in the z direction and which is also uniform in the y direction. In order to more accurately apply the preceding theory to tokamak experiments, we have extended the mode conversion problem to a new slab geometry which more closely matches the magnetic field and geometry features of a toroidally-shaped plasma. The most important change was to give the FAW a nonzero poloidal wavenumber, since the incident FAW does not have an infinite extent in the poloidal direction. Additionally, we have included a poloidal magnetic field, which changes as the wave propagates.

The mode conversion region is approximately described by a set of Cartesian coordinates, with the x direction chosen along the equatorial plane of the torus and the y and z directions corresponding to the poloidal and toroidal directions, respectively. In this model, the density and magnetic field of the plasma will still vary only in the x direction. Since a real tokamak has both a toroidal and poloidal mag-

[14] A.K. Ram and A. Bers, *Phys. Fluids* B3: 1059 (1991).

netic field, the magnetic field vector lies in the y-z plane, forming an angle $\alpha(x)$ with the z axis. To calculate the dispersion relation for fast Alfvén waves, we rotate the coordinate frame into the direction of the magnetic field, so that at each point x the coordinates must be rotated by $\alpha(x)$.

The electric field of the FAW is assumed to have the form

$$\vec{E} = \hat{E}(x)\ \exp(ik_y y + ik_z z - i\omega t) \tag{1}$$

where k_y and k_z correspond to the poloidal and toroidal wavenumbers, respectively. Each wavenumber is treated as a constant in the vicinity of the mode conversion region. Then, in the rotated coordinate system, the wavenumbers become

$$k_{\|} = k_y \sin\alpha + k_z \cos\alpha \tag{2}$$

$$k_{+} = k_y \cos\alpha - k_z \sin\alpha \tag{3}$$

The dispersion relation of the fast Alfvén wave is then calculated from cold plasma theory, using the approximation that for a low frequency wave, the electric field in the direction of the equilibrium magnetic field will be shorted out. Under these conditions, the propagation of the FAW is described by a second-order differential equation for $E = E_+$, of the form

$$\frac{d^2E}{d\xi^2} + p(\xi)\frac{dE}{d\xi} + q(\xi)E = 0 \tag{4}$$

with the potential functions

$$p(\xi) = \frac{d}{d\xi}\ln\left(\frac{S - n_{\|}^2}{S - n_{\|}^2 - n_{+}^2}\right) \tag{5}$$

and

$$q(\xi) = S - n_{\|}^2 - n_{+}^2 - (\alpha')^2 \tag{6}$$

$$- \frac{D^2 - n_+D' - \alpha' n_{\|}D + \alpha'' n_{\|}n_+}{S - n_{\|}^2} - \frac{S'(n_+D - \alpha' n_{\|}n_+)}{(S - n_{\|}^2)(S - n_{\|}^2 - n_{+}^2)}$$

In this notation, ξ is once again $(\omega/c)x$, and the primes all indicate differentiation with respect to ξ. S and D are the usual cold plasma tensor elements.

In our previous mode conversion analysis, all resonant dissipation occurred at the ion-ion hybrid resonance, which is the point at which $S - n_{\|}^2 = 0$. The most interesting feature of this new theory is the appearance of a second singularity in the functions p and q, at the point in space where $S - n_{\|}^2 - n_{+}^2 = 0$. This has been observed in other mode conversion theories with similar features.[15] For comparison to our theory of the preceding section, consider the change of variables

$$E(\xi) = \exp\left(-\frac{1}{2}\int p(\xi)\,d\xi\right)W(\xi)$$

$$= \sqrt{\frac{S - n_{\|}^2 - n_{+}^2}{S - n_{\|}^2}}\ W(\xi) \tag{7}$$

which results in the equation

$$\frac{d^2W}{d\xi^2} + Q(\xi)W = 0 \tag{8}$$

where $Q(\xi) = q(\xi) - (1/2)p(\xi)' - (1/4)p(\xi)^2$ In figure 6, the new potential function Q is plotted and compared to the potential for $n_+ = 0$.

[15] R.B. White and F.F. Chen, *Plasma Phys.* 16: 565 (1974); T.H. Stix, *Waves in Plasmas* (New York: American Institute of Physics, 1992), pp. 369-379.

In this more complicated problem, numerical integration of the equation (4) is used to compare to the much simpler Budden mode conversion solution.[16] For comparision, the functions (5) and (6) were fit to simpler expressions in a few parameters:

$$p(\xi) = \frac{1}{\xi} - \frac{1}{\xi - \xi_r} \tag{9}$$

$$q(\xi) = \gamma - \frac{\beta}{\xi} + \frac{\delta}{\xi(\xi - \xi_r)} . \tag{10}$$

These parameters were chosen to fit the features of TFTR during mode-conversion heating experiments.[17]

Figure 7 shows the numerically calculated values of the power mode-conversion coefficient, for increasing values of k_+. It is observed that for k_+ greater than 8 m^{-1}, the fraction of wave power dissipated in the resonant region increases significantly, to well beyond the Budden limit of 25 percent. For comparison, we also graph the predicted mode conversion from Budden theory, which is T(1-T), where T is the power transmitted through the resonant region.

In order to understand the nature of this additional dissipation, we can check the conservation of wave power directly from the numerically integrated solution of (4). The results are plotted in figure 8 in the region of the resonances. For $k_+ = 4\ m^{-1}$, there is only one point where FAW power has a significant change, at the usual ion-ion hybrid resonance $S - n_\parallel^2 = 0$. However, for $k_+ = 15\ m^{-1}$, there is also power lost from the FAW at the second resonant point where $S - n_\parallel^2 - n_\perp^2 = 0$. This appears to indicate that the increased power dissipation which is observed in figure 7 occurs at the second resonance. This result may mean that the additional power may be lost to some process other than mode conversion to IBWs. We are currently trying to understand this new result.

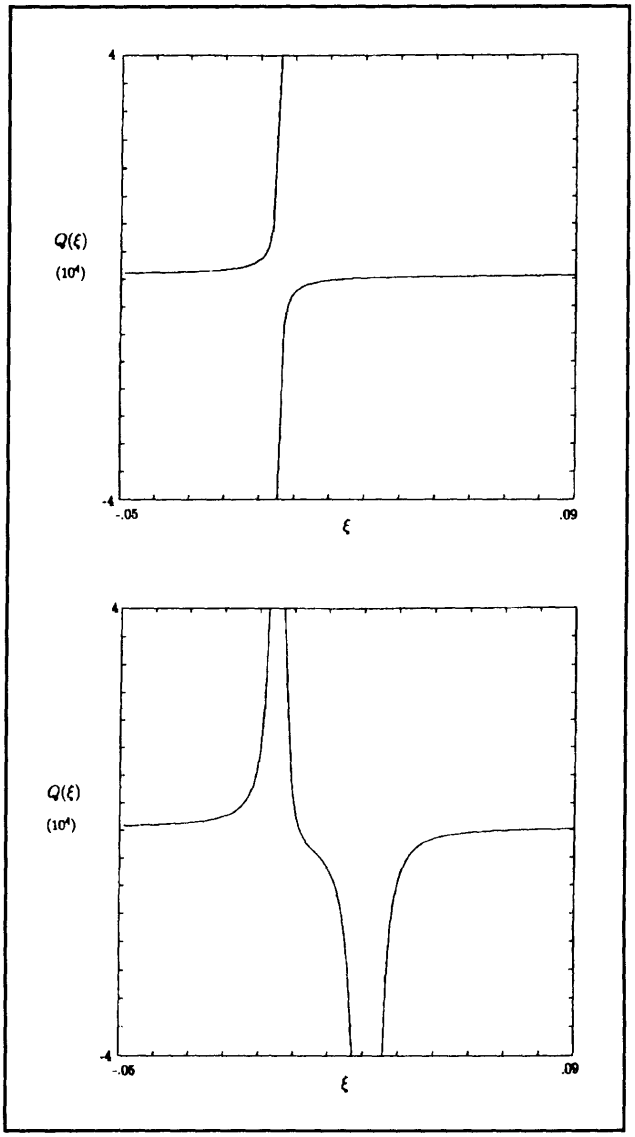

Figure 6. $Q(\xi)$ in vicinity of mode-conversion region for (a) $k_+ = 0$ and (b) $k_+ = 15\ m^{-1}$.

[16] K.G. Budden, *The Propagation of Radio Waves* (Cambridge: Cambridge University Press, 1985), pp. 596-602.

[17] R. Majeski et al., in *Proceedings of the 11th Topical Conference on RF Power in Plasmas*, Palm Springs, California, 1995, ed. R. Prater and V.S. Chan (New York: American Institute of Physics Conference Proceedings 355, 1995), p. 63.

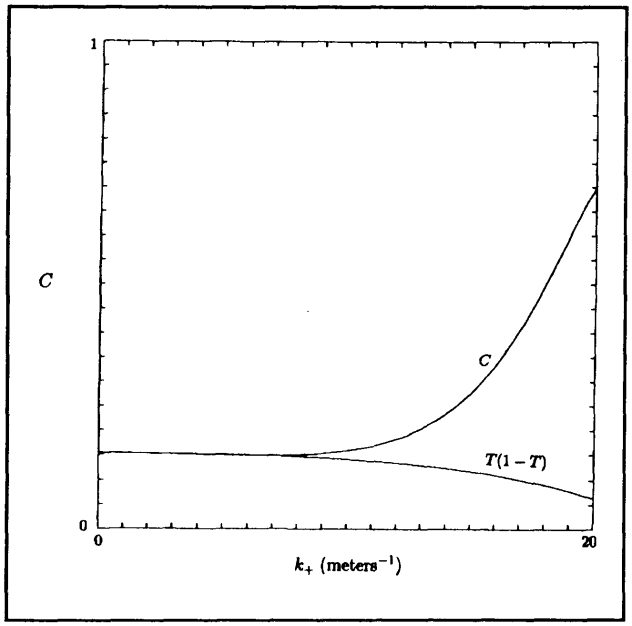

Figure 7. Fraction of FAW power dissipated (C) and Budden prediction [T(1 – T)] as a function of k_+ for TFTR parameters.

1.2.4 Enhancement of the Bootstrap Current in Tokamaks Using RF Waves

Sponsors

National Science Foundation
Grant ATM 94-24282
U.S. Department of Energy
Grant DE-FG02-91-ER-54109

Project Staff

Steven D. Schultz, Professor Abraham Bers, Dr. Abhay K. Ram, Dr. Joachim Theilhaber

In *Progress Report No. 137*, we began considering the use of radio frequency (RF) waves to enhance the bootstrap current to create a sustained plasma current in tokamak devices. This analysis used kinetic theory to determine the effects of a toroidal shape (see figure 9) and quasilinear diffusion on the velocity-space distribution of electrons.

The current carried by electrons (including bootstrap current) can be found by taking a moment of their distribution function f,

$$J_{||} = -e\int d^3v\, v_{||} f. \qquad (1)$$

We take f to be at steady state, averaged over the magnetic gyromotion, and independent of the toroidal angle ϕ by axisymmetry. Under these

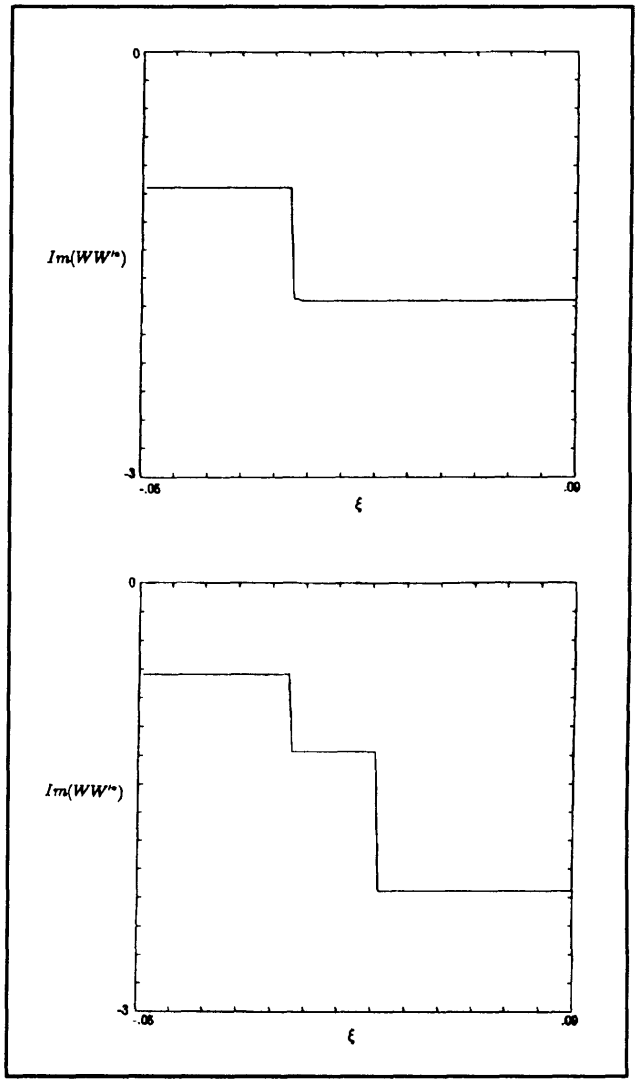

Figure 8. FAW power as a function of ξ in the mode-conversion region, showing changes at the resonances.

assumptions, f can be written as a function of the guiding center coordinates r and θ and two constants of the motion, the electron's energy E and magnetic moment μ. Then f satisfies the *drift kinetic equation* (DKE)

$$v_{||}\frac{B_\theta}{B}\frac{1}{r}\frac{\partial f}{\partial \theta} + v_{D_r}\frac{\partial f}{\partial r} = C(f) + Q(f). \qquad (2)$$

where C(f) is the collision operator, and Q(f) is the quasilinear operator for diffusion due to RF waves.

In *Progress Report No. 137*, we showed one way of solving (2) through expansion in small parameters. The result was

$$f = f_0^{(0)} - \frac{m}{eB_0} v_{||}\frac{\partial f_0^{(0)}}{\partial r} + \bar{f}_1^{(0)} \qquad (3)$$

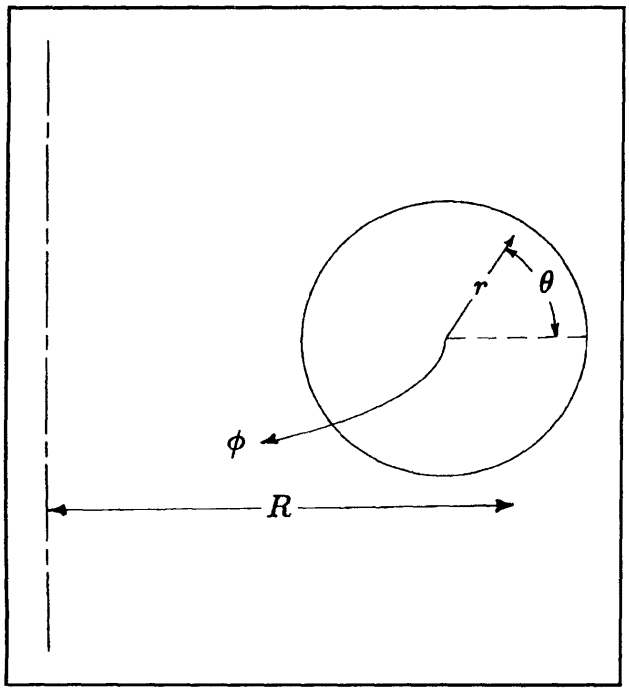

Figure 9. Toroidal coordinate system.

The modified electron distribution due to RF effects only was the solution to

$$\left\{C(f_0^{(0)}) + Q(f_0^{(0)})\right\} = 0 \qquad (4)$$

where the braces indicate averaging over a bounce orbit. Inclusion of guiding center drifts gives the higher order equations found in *Progress Report No. 137*. Their solution gives the second quantity in (3) as well as the bounce-averaged quantity $\bar{f}_1^{(0)}$, which is found to be the solution to

$$\left\{C(\bar{f}_1^{(0)}) + Q(\bar{f}_1^{(0)})\right\} = S \qquad (5)$$

with the "source term"

$$S \equiv \left\{ C\left(\frac{m}{eB_0} v_{\|} \frac{\partial f_0^{(0)}}{\partial r} \right) + Q\left(\frac{m}{eB_0} v_{\|} \frac{\partial f_0^{(0)}}{\partial r} \right) \right\} \qquad (6)$$

Since the remainder of a quantity after bounce averaging is generally smaller by a factor of r/R_o (the ratio of minor radius to major radius), the θ-dependent contribution $f_0^{(1)}$ (described in *Progress Report No. 137*) has been neglected in subsequent derivations.

The kinetic solution for the bootstrap current is thus dependent upon our ability to find solutions $f_0^{(0)}$ and $\bar{f}_1^{(0)}$ for the similar equations (4) and (5). Analysis of this type of quasilinear/Fokker-Planck equation has been important in RF current drive theory. Due to the complexity of the Fokker-Planck collision operator, numerical solutions have proved to be very useful in this analysis.[18] In our work, we have used a simple Fokker-Planck computer code which makes use of a linear collision operator with only pitch angle collisions. This limited operator is sufficient for bootstrap analysis, since it is the deflection of the electrons' path with respect to the magnetic field which moves them into and out of trapped orbits, transferring momentum to the passing electrons and producing the bootstrap current.

This type of collisional/quasilinear code requires a large amount of storage space and run time. Optimization of the code has therefore been an important task. The use of parallel processing machines is also being considered to allow the use of more complicated Fokker-Planck operators or, as a more advanced problem, to solve the DKE (2) in four dimensions without resorting to the small-parameter expansion discussed above.

While this kinetic analysis is useful for its approach to RF velocity-space diffusion, it is important to consider the approach to the bootstrap current used in neoclassical transport theory.[19] In particular, the diffusion of plasma across the magnetic field as the driving source of the bootstrap current must be considered. As shown in these theories, the friction force felt by particles moving parallel to the magnetic field is directly related to both cross field neoclassical transport and the bootstrap current. An important consideration in our enhancement of the current may be a possible effect on plasma confinement due to increased diffusion. The transport theories[19] are all based on the approximation that the distributions of all species are close to a Maxwellian, which may not be accurate in the case of RF-modified plasmas. So we have considered the generalization of transport theories to non-Maxwellian plasmas as a future step in this problem.

Once the proper codes have been developed or adapted to solve the problem, the quasilinear oper-

[18] J. Killeen, G.D. Kerbel, M.G. McCoy, and A.A. Mirin, *Computational Methods for Kinetic Models of Magnetically Confined Plasmas* (New York: Springer-Verlag, 1986).

[19] S.P. Hirshman and D.J. Sigmar, *Nucl. Fusion* 21: 1079 (1981); F.L. Hinton and R.D. Hazeltine, *Rev. Mod. Phys.* 48: 239 (1976).

ator can be changed to model any of the well-known types of RF waves (lower hybrid, fast Alfvén, electron cyclotron, or ion-Bernstein). By changing the frequency and wavenumber characteristics of these waves, the velocity-space diffusion of the distribution function can be controlled. Comparision of the numerically generated results of the code will be used to find a RF wave scheme which can produce enhanced values of the bootstrap current.

1.2.5 ICRF-Heated Trapped Particles and Banana Widening Transport

Sponsor

U.S. Department of Energy
Grant DE-FG02-91-ER-54109

Project Staff

Luigi Vacca, Professor Abraham Bers, Dr. Abhay K. Ram

As shown in *Progress Report No. 137,* the resonant minority ions mostly gain perpendicular energy from the fast Alfvén wave by localized kicks in phase space occuring at the resonant layer location. It has been observed experimentally that the resonant trapped particles' banana tips are very close to the resonance layer.[20] In this report, we provide a theoretical explanation for the occurence of the resonant trapped ions' banana tips near the resonant layer. In addition, we describe the loss of the resonant trapped ions due to widening of their banana orbits as they are heated by the RF fields. The occurence of the banana tips near the resonant layer can be explained in terms of diffusion in velocity space due to wave-particle resonance. In the case of ICRF heating, the increase in perpendicular energy is much greater than the increase in parallel energy

$$|\delta v_{\parallel}|^2_{RF} << |\delta v_{\perp}|^2_{RF}. \tag{1}$$

The ion parallel velocity is a function of space for a single particle orbit. If we neglect the drifts, the parallel velocity can be written as

$$v_{\parallel} = \pm\left[\frac{2}{m}(E - \mu B_0 + \varepsilon\mu B_0)\right]^{1/2}\left(1 - k^2 \sin^2\frac{\theta}{2}\right)^{1/2} \tag{2}$$

where k^2 is the trapping parameter given by

$$k^2 = \frac{2\varepsilon\mu B_0}{E - \mu B_0 + \varepsilon\mu B_0}. \tag{3}$$

E is the total energy, μ is the magnetic moment, and $\varepsilon = r/R_0$ where r is the minor radius and R_0 is the major radius. Trapped particles have trapping parameters greater than unity: $k^2 > 1$. The trapping parameter also yields the poloidal angle of the banana tips

$$\theta_{tip} = 2\sin^{-1}\left(\frac{1}{k}\right). \tag{4}$$

It is evident from (4) that when k^2 increases, θ_{tip} decreases and vice versa. When the poloidal angle of the banana tip decreases, the trapped particle becomes more trapped. We show that this is exactly what happens when a trapped particle gains energy from the RF field. First, we establish a relationship for the increase in energy with increase in magnetic moment. Consistent with (1), the total increase in energy is equivalent to the total increase in perpendicular energy; thus

$$\delta\mu \sim \frac{\delta E}{B_{res}} \tag{5}$$

where B_{res} is the magnitude of the magnetic field at the resonance point. Using (3), the variation of k^2 yields

$$k^2 + \delta k^2 = \frac{2\varepsilon(\mu + \delta\mu)B_0}{D + \delta\mu(B_{res} - B_0 + \varepsilon B_0)} \tag{6}$$

where $D = E - \mu B_0 + \varepsilon\mu B_0 > 0$. After some algebra, we find

$$[1 + \delta\mu(B_{res} - B_0 + \varepsilon B_0)/D]\frac{\delta k^2}{k^2} =$$

$$\frac{\delta\mu}{\mu}[1 - \mu(B_{res} - B_0 + \varepsilon B_0)/D]. \tag{7}$$

If $\delta\mu > 0$, then $\delta k^2 > 0$ if

$$[1 - \mu(B_{res} - B_0 + \varepsilon B_0)/D] > 0. \tag{8}$$

Manipulating inequality (8) yields equivalently

$$E - \mu B_{res} > 0. \tag{9}$$

---

[20] G.W. Hammett, *Fast Ion Studies of Ion Cyclotron Heating in the PLT Tokamak,* Ph.D. diss., Princeton University, 1986.

Equation (9) is satisfied for all trapped particles that intersect the resonance layer. When the trapped minority ion gains perpendicular energy, its banana tips move toward the resonance layer. If the minority ion orbit does not intersect the resonant layer, it does not interact with the wave, and, therefore, its banana tips do not move. This simplified model does not account for collisions and Doppler-shifted resonance which produces diffusion in parallel velocity. However, for highly energetic ions, collisions are rare and the ion moves eventually with its tips toward the resonant layer. Once the particle tips have reached the resonance layer, they can move along it if we then account for the parallel momentum exchanged with the wave. Collisional energy transfer from the energetic minority ions to bulk electrons and ions also induces a poloidal and radial displacement of their banana tips. The radial movement of the tips and the pitch-angle scattering occur on a slower time scale than the angular movement of the banana tips given by (7). In a strong RF-heating regime where pitch-angle scattering is not fast enough to make the resonant distribution function isotropic, most of the resonant ions become trapped with their banana tips in the resonance layer region. For this reason, the resonant ion distribution function is essentially comprised of trapped ions.

Loss of Resonant Banana Particles

Resonant trapped ions whose banana tips are on the resonant layer also have their banana widths increase as their energy increases with time. If the banana orbits have widths comparable to the tokamak minor radius, then the outer leg of the banana orbit touches the edge of the plasma and they become unconfined. This mechanism of transport differs from those previously provided on this subject.[21] To study this effect, we focus on the resonant trapped particles that are barely confined. Our approach assumes that the loss of the barely confined particles takes place in a steady-state mode where the ion distribution function shape is practically unchanged. The steady-state scenario can be described by the lost, barely confined particles being continuously replaced by other resonant ions diffusing in phase-space, and being globally replaced by a source of heated minority ions.

We find that the radial displacement δx along the equatorial plane always increases with increasing magnetic moment and is larger for particles whose banana tips are close to the plasma's edge along the resonance layer. We find

$$\delta x = \frac{1}{A_c^2} \frac{\delta\bar{v}^2(1 + a_r/R_0)^2 - \delta\bar{\mu}(1 + a_r/R_0) + 2A_c(1 - x_0^2)\delta\bar{p}}{D(x_0, \theta_0)} \tag{10}$$

where $A_c = \mu_0 q I_{tor}/4\pi m v_{th}$, $\bar{v}^2 = v^2/v_{fh}^2$, $\bar{\mu} = 2B_0\mu/mv_{fh}^2$, $\bar{p} = A_\xi^2 x_{fp}^2$, $x = r/a_r$, a_r is the minor radius of the tokamak, and x_0, θ_0 are respectively the radial and poloidal coordinates of the banana tips. The denominator is given by

$$D(x_0, \theta_0) = 4(1 - x_0^2) + \left[-1 + \frac{a_r}{R_0}(x_0 \cos\theta_0 - 2) \right] \cdot \frac{(1 - x_0^2)^2}{[1 + (a_r/R_0)](1 - x_0 \cos\theta_0)} . \tag{11}$$

The denominator of (10) is always positive for the trapped particles that intersect the resonant layer. The direction of the radial displacement δx is outward for a positive numerator and inward for a negative numerator. The changes in the phase-space variables caused by cyclotron resonance satisfy the following relations

$$\delta\bar{v}^2 = \frac{\delta\bar{\mu}}{h_{res}} + 2|\bar{v}_{||}|_{res}\delta\bar{v}_{||} \tag{12}$$

where $h_{res} = 1 + (a_r/R_0)\cos(\theta)$ at the resonance location and

$$\delta\bar{p} = -h_{res}\,\delta\bar{v}_{||} \tag{13}$$

where the subscript res refers to the resonance location. The radial velocity of trapped minority ions due to a change in magnetic moment is given by

[21] G.W. Hammett, *Fast Ion Studies of Ion Cyclotron Heating in the PLT Tokamak*, Ph.D. diss., Princeton University, 1986; L. Chen, J. Vaclavik, and G. Hammett, "Ion Radial Transport Induced by ICRF Waves in Tokamaks," *Nucl. Fusion* 28: 389 (1988).

$$< V_r > = < \frac{\delta x}{\delta t} > =$$

$$\frac{a_r}{A_c^2} \frac{< \delta\hat{\mu} > \left[\frac{(1 + a_r/R_0)^2}{h_{res}} - (1 + a_r/R_0) \right]}{T_{btrapp} D(x_0, \theta_0)} \quad (14)$$

where we used the average change in radial coordinate in one poloidal period and let $\delta t = T_{btrapp}$, where T_{btrapp} is the poloidal bounce time for trapped particles. Also, $< \delta\bar{\mu} >$ is the average change in magnetic moment that the particle experiences in one poloidal period. This velocity can be compared to the drift velocity of banana tips when the wave spectrum is asymmetric.[20] The radial velocity of trapped minority ions due to a change in magnetic moment is given by (14) where we used the average change in radial coordinate in one poloidal period and let $\delta t = T_{btrapp}$. Also $< \delta\bar{\mu} >$ is the average change in magnetic moment that the particle experiences in one poloidal period. This velocity can be compared to the drift velocity of banana tips when the wave spectrum is asymmetric

$$\left| \frac{< V_{tip} >}{< V_r >} \right| \sim \left| \frac{10N A_c^2 q_s D(x_0, \theta_0)}{(\omega_{c0} t_b)^2} \right| . \quad (15)$$

For instance, let's take D~3 and N~10; then this ratio is smaller than unity for typical tokamak parameters.[22] In the case of small-width banana orbits, D≪1, the ratio in (15) is even smaller.

We can also compute the power lost by introducing a model distribution function for their resonant trapped ions:

$$f(x, \bar{v}) = \frac{N_{res}}{2\pi a R_0^2} g(\gamma_n, \gamma_T)(1 - x^2)^{\gamma_n} \frac{M}{2\pi T_{eff}}^{3/2} e^{-Mv^2/2T_{eff}} \frac{2}{\sqrt{\pi}} \frac{\exp[-(\psi^2/\delta\psi^2)]}{\delta\psi} \quad (16)$$

where N_{res} is the total number of resonant trapped ions in the vicinity of resonant layer, γ_n and γ_T are the density and temperature profiles parameters, T_{eff} is the minority tail temperature, ψ is the pitch-angle at the resonant layer, and

$$g(\gamma_n, \gamma_T) = \frac{1}{(1/\sqrt{2})[(60/9)(1/A_c^2)]^{3/4} \int_0^1 dx (1 - x^2)^{\gamma_n + (3/4)(\gamma_T - 2)}} \quad (17)$$

gives the proper normalization for $f(x, \bar{v})$. The distribution function is bi-Maxwellian in energy and pitch-angle. The spread in pitch-angle space $\delta\psi \sim \sqrt{\nu_{ii}\tau_s}$ is a function of pitch-angle scattering frequency ν_{ii} and drag time τ_s. The energy lost can be computed by estimating the number of particles that cross the plasma boundary in a poloidal period. The ratio of the maximum energy lost to the total minority energy content is

$$\frac{\text{Maximum energy lost}}{\text{Total energy content}} \sim$$

$$\frac{\int dV \int_{v_b^2 - \delta v_{max}^2}^{v_b^2} \int_{-\delta\psi}^{\delta\psi} d\psi \, dv \, 2\pi v^2 \, f \, mv^2/2}{\int dV \int_0^{v_b^2} \int_{-\delta\psi}^{\delta\psi} d\psi \, dv \, 2\pi v^2 \, f \, mv^2/2} \quad (18)$$

[22] I.H. Hutchinson, et. al., "First Results From Alcator C-Mod," *Phys. Plasmas* 1: 1511 (1994).

where dV is the volume that comprises the resonant ions, $v_b^2=9A_c^2v_{th}^2/4$, and δv_{max}^2 is the positive kick in energy gained by a resonant particle in one semi-poloidal period. The power dependence in (18) is given by $T_{eff}=P_{RF}\tau_s/3n_m$, where P_{RF} is the RF power density and n_m is the minority density. The range of the velocity space integral is over all particles that are deconfined due to RF; v_b^2 is the energy of an ion which in the absence of P_{RF} is confined, but which in the presence of P_{RF} gains an energy δv_{max}^2 that will deconfine it. The maximum kick in energy is computed by integrating the equation of motion in the vicinity of the plasma layer where most absorption takes place, using the results shown in *Progress Report No. 137.*

We numerically compute the power lost adopting the following tokamak parameters: minor radius a=0.30 m, inverse aspect-ratio $a/R_0=1/3$, majority temperature is 1 KeV, and minority density is 10^{18} m^{-3}; and we plot the power loss for three different values of the toroidal current I: 1.3 MA, 1.5 MA, and 2 MA, respectively. The result is shown in figure 10, where we can point out that the loss of the resonant minority ions is negligible at low powers, but becomes relevant at high powers, namely $P_{RF} > 3$ MW. The increase in energy loss due to an increase in RF power is substantial at low current (see the plot for I = 1.3 MA), because there are more energetic ions that touch the plasma edge. As is well known, an increased RF power injected into the plasma requires higher toroidal currents to keep the energetically-produced resonant ions confined.

The dependence of the energy loss on the toroidal current is due to A_c, which appears in the velocity integral limits. The explicit dependence of the fluxes on the total RF power is the new and main result of this report. We also point out that the same approach can be applied to the future study of resonating alpha particles confinement in a tokamak. Further details of this calculation and other aspects of ICRF heating are being written up in a forthcoming Ph.D. dissertation.[23]

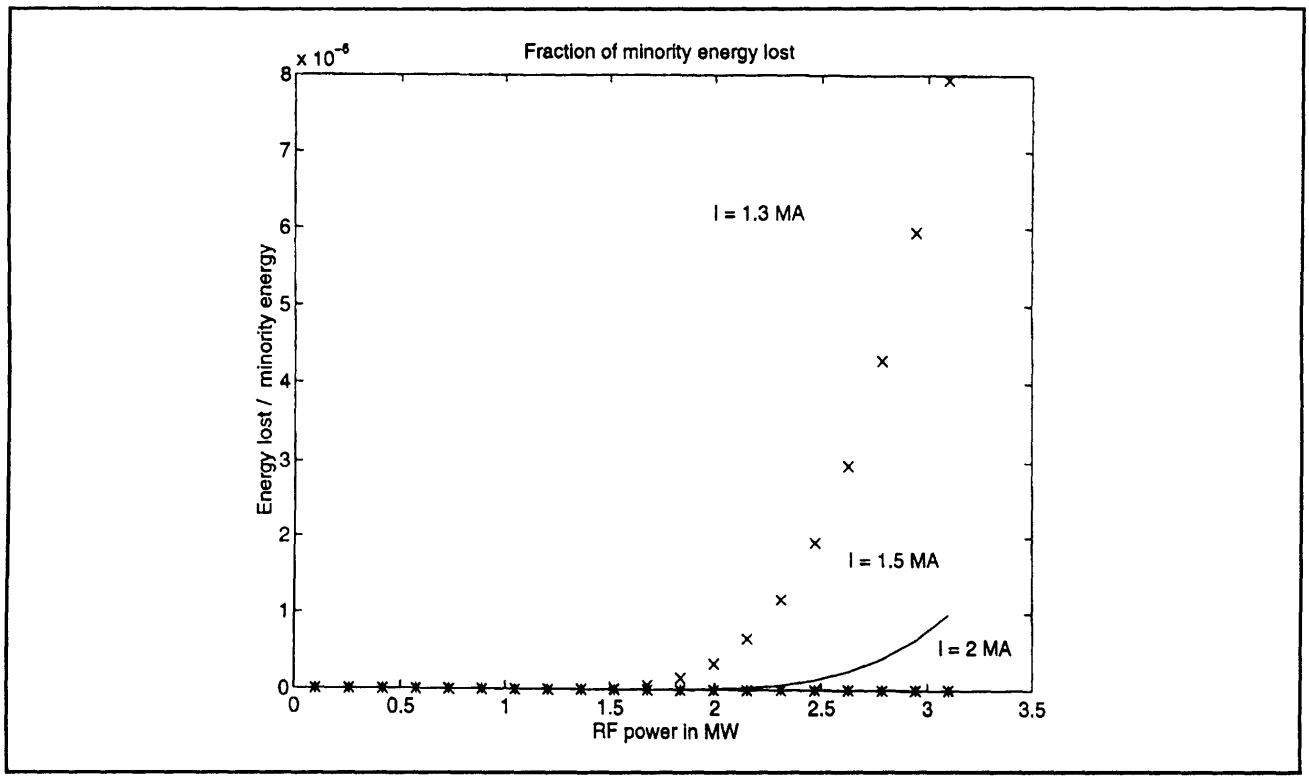

Figure 10. Ratio minority energy loss to the total energy of the minority species as function of the total RF power for standard Alcator C-Mod parameters[22] and for three different values of the toroidal current. The full line refers to a toroidal current of 1.5 MA; the * line refers to a toroidal current of 2 MA, and the x line refers to a toroidal current of 1.3 MA.

[23] L. Vacca, *RF-Induced Transport of Resonant Minority Species in ICRF-Heated Tokamaks*, Ph.D. diss., Dept. of Nuclear Eng., MIT, 1996.

1.2.6 Plasma Wave Induced Stochasticity in a Magnetic Field

Sponsor

National Science Foundation
Grant ECS 94-24282

Project Staff

Felicisimo W. Galicia, Dr. Abhay K. Ram, Professor Abraham Bers

In a magnetized plasma, the motion of a charged particle under the influence of an electrostatic wave that propagates across the magnetic field is a long-standing problem in chaotic dynamics whose detailed solution for various applications (e.g., plasma wave heating, particle acceleration) remains incomplete. Our recent work on this problem concentrated on the so-called web stochasticity analysis as a means of predicting the stochastic dynamics in this system.[24] Our current research has refocused efforts on the role that the Chirikov island overlapping condition can play in determining a threshold for stochasticity. The use of the Chirikov condition in the on-resonance case (the wave frequency $\omega = n\Omega$ where Ω is the cyclotron frequency) first appeared in the work of Fukuyama, et al.[25] They derived analytic thresholds for stochasticity valid for high harmonics ($n \gg I$, where I is the action) and energies. Methods motivated by the Chirikov condition for the off-resonance case have been studied by Karney[26] and again, this work is valid for high harmonics and energies.

The goal of our current research is to determine a threshold for stochasticity valid for both the on- and off-resonance cases at low and high energies. To this end, our strategy has been to analyze previous analytical and computational work and to look for possible extensions and generalizations. The full Hamiltonian describing the system after appropriate transformations and normalizations has the form:

$$H = \frac{I}{T} + \varepsilon \sum_n J_n(\sqrt{2TI}) \cos(n\psi - \tau) \qquad (1)$$

where T is the ratio of the frequency of the perturbing plasma wave to the cyclotron frequency and ε is a dimensionless non-linearity parameter. At high harmonics and energies, expansions of the Bessel functions lead to tractable, approximate solutions complemented by results from computations;[26] unfortunately, these solutions are not applicable at lower energies and harmonics. Karney's method is to take an analytical expression for the threshold of primary island formation and to extend it to an upper bound for stochasticity in an ad hoc manner; numerical results are used to justify this extension. Karney's upper bound takes the form:

$$\varepsilon = \frac{\pi^{1/2} 2^{1/4} I^{3/4}}{4nT^{5/4}} \qquad (2)$$

where n is the nearest integer to T. Also, by limiting the stochastic regime from below to those regions of action in phase space which have enough energy to be trapped by the perturbing wave, Karney determines a lower bound which takes the form:

$$\varepsilon = \frac{2I}{T} - \sqrt{\frac{8I}{T}} + 1. \qquad (3)$$

A wave amplitude threshold for stochasticity (ε_{th}), as well as the action at which it sets in (I_{th}), may be found by the simultaneous solutions of (2) and (3).

A comparison of Karney's bounds to computer simulations is included in figures 11-16. Figure 11 is a surface plot of the upper bound in action of the stochastic region in phase space, as the non-linearity parameter ε and the frequency ratio T are varied where T is near 30. The upper bound is determined numerically by integrating the equations of motion and examining trajectories in phase space. Karney's work predicts an almost flat surface for such a plot. However, the surface in figure 11 is more complex. The surface shows more sensitivity to the nearness to resonance than that predicted by Karney. Figures 12-16 compare sections of the surface in figure 8 at constant T with Karney's threshold. The computer data is represented by the points and the predicted bounds are represented by the curves. These plots further support the need to increase the sensitivity of Karney's upper bound to the nearness to resonance.

---

[24] A. Bers, et. al., "Plasma Wave Interactions—RF Heating and Current Generation," *RLE Progress Report* 135: 184 (1992); 136: 240 (1993).

[25] A. Fukuyama, M. Momota, R. Itatani, and T. Takizuka, *Phys. Rev. Lett.* 28: 701 (1977).

[26] C.F.F. Karney, *Phys. Fluids* 21: 1584 (1978); 22: 2188 (1979).

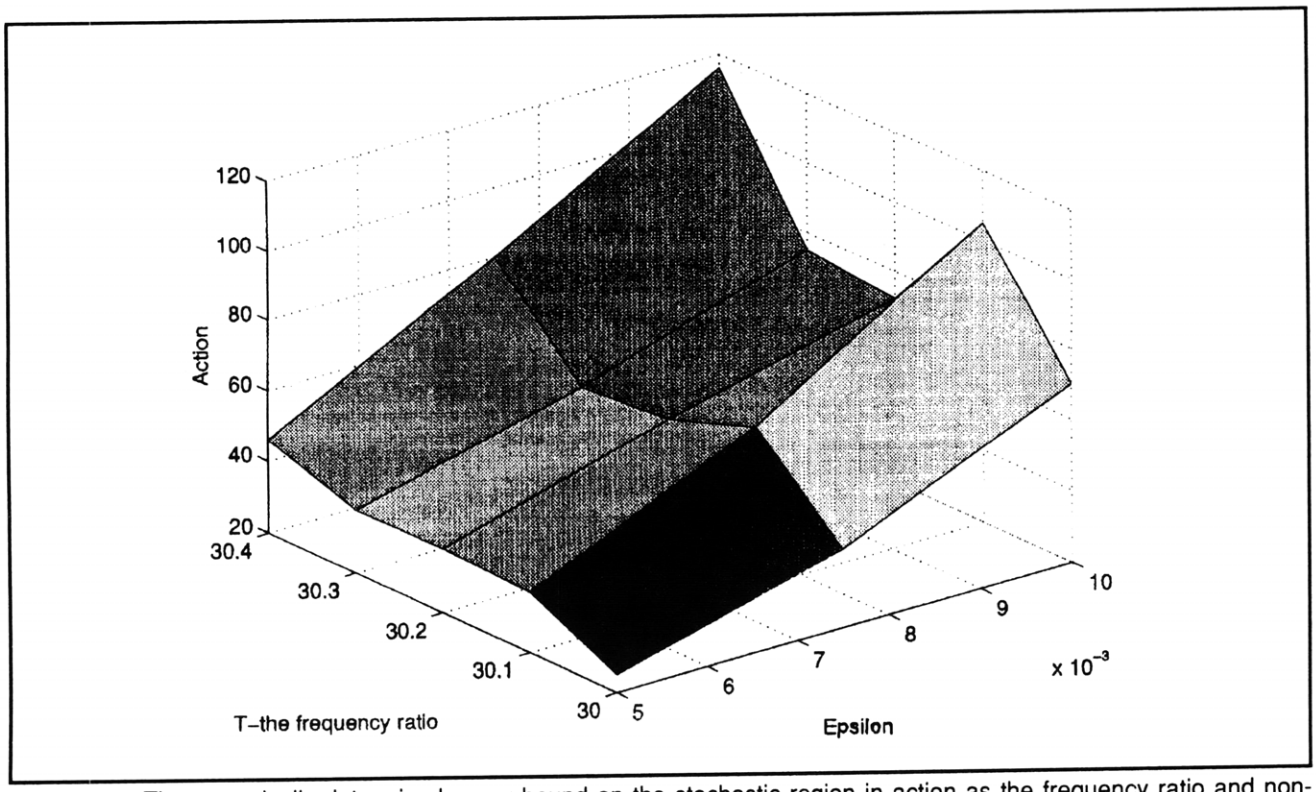

Figure 11. The numerically determined upper bound on the stochastic region in action as the frequency ratio and nonlinearity parameter are varied for a frequency ratio near 30.

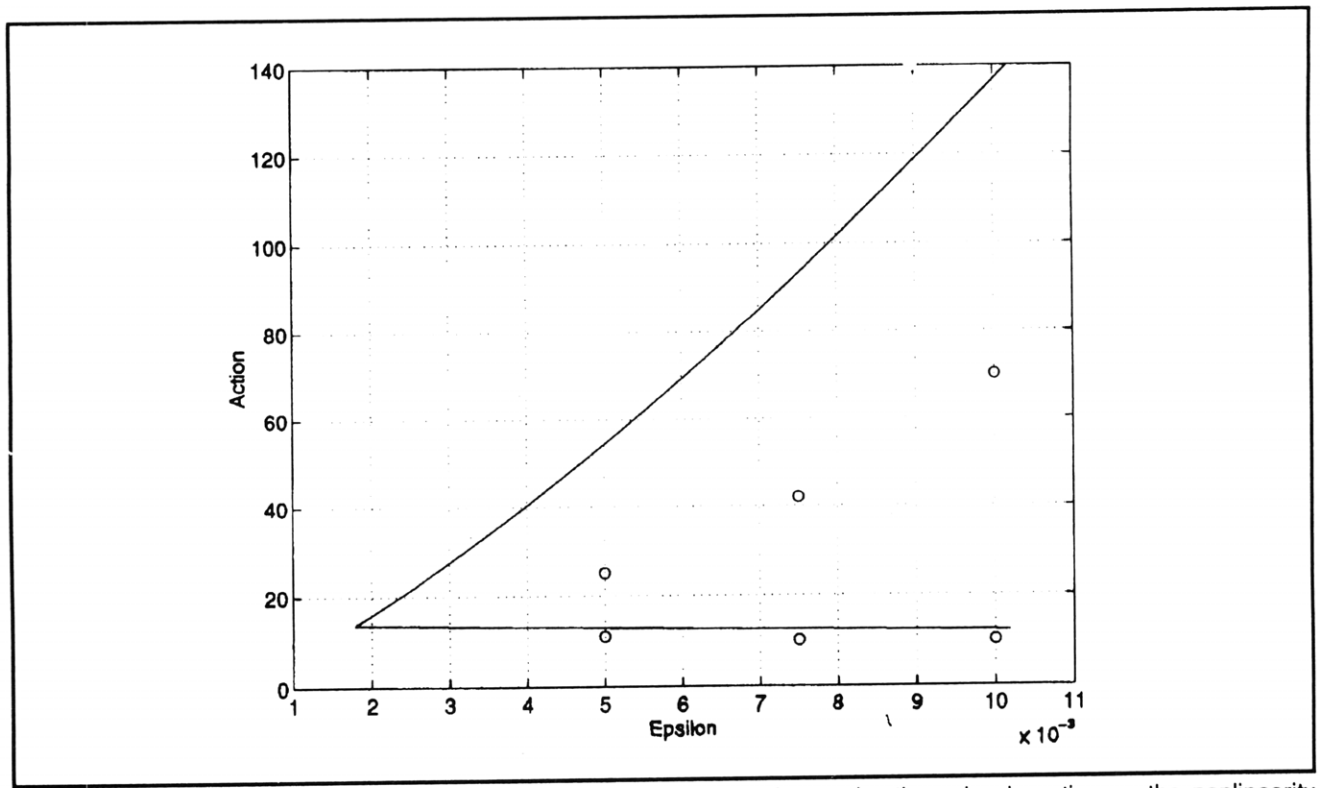

Figure 12. The numerically determined upper and lower bound on the stochastic region in action as the nonlinearity parameter is varied for a frequency ratio of 30.

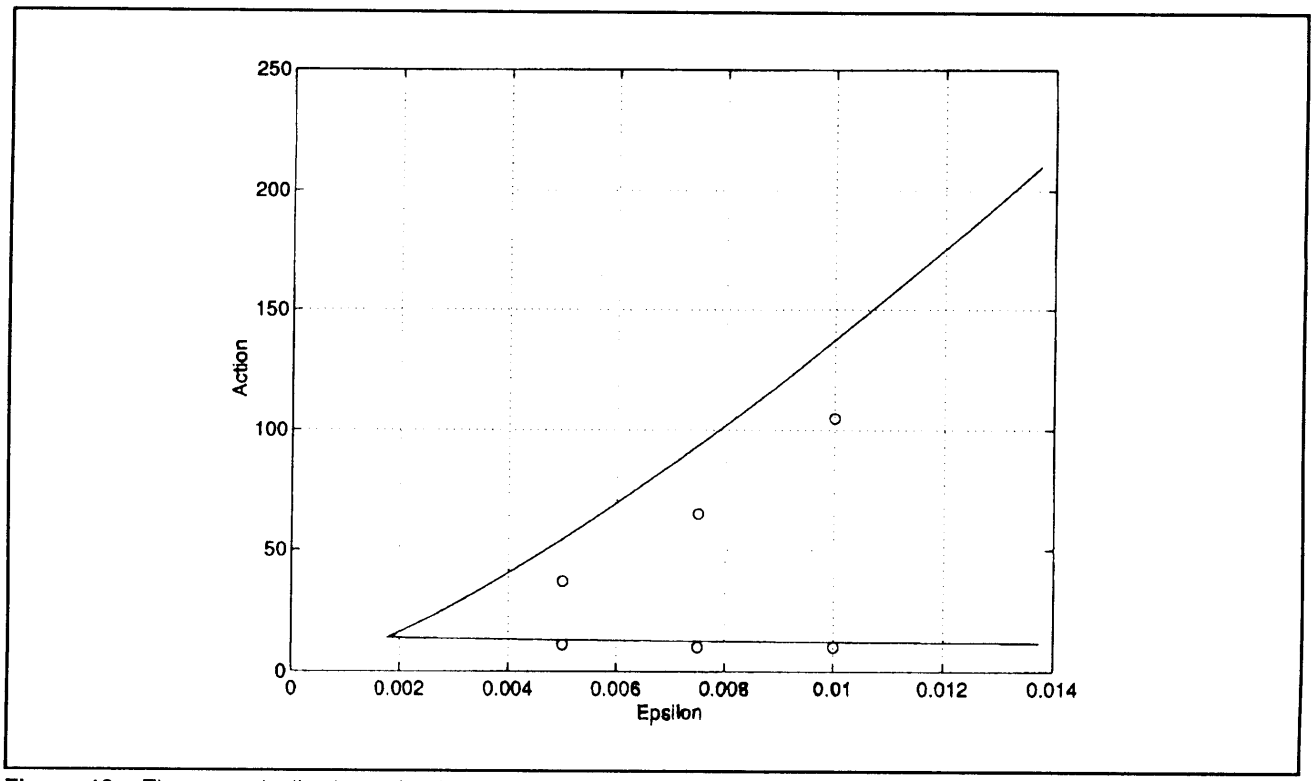

Figure 13. The numerically determined upper and lower bound on the stochastic region in action as the nonlinearity parameter is varied for a frequency ratio of 30.1.

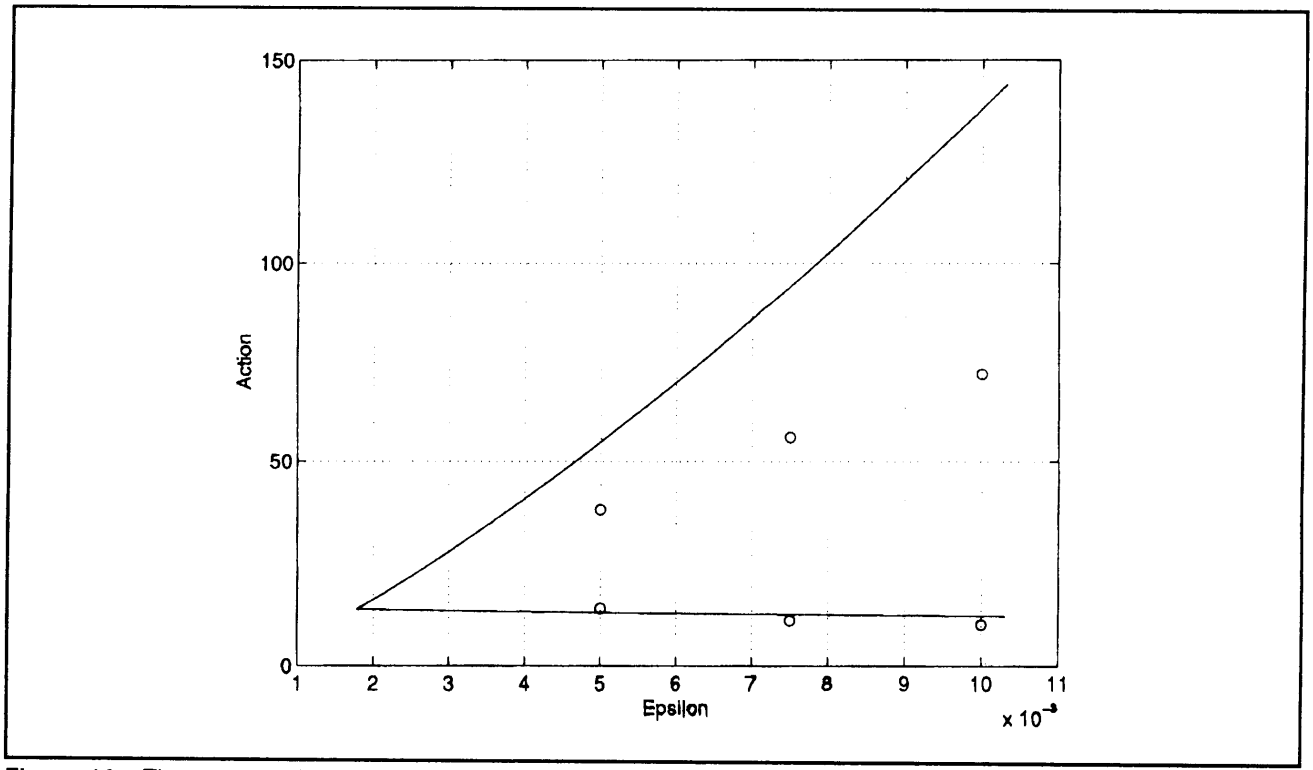

Figure 14. The numerically determined upper and lower bound on the stochastic region in action as the nonlinearity parameter is varied for a frequency ratio of 30.2.

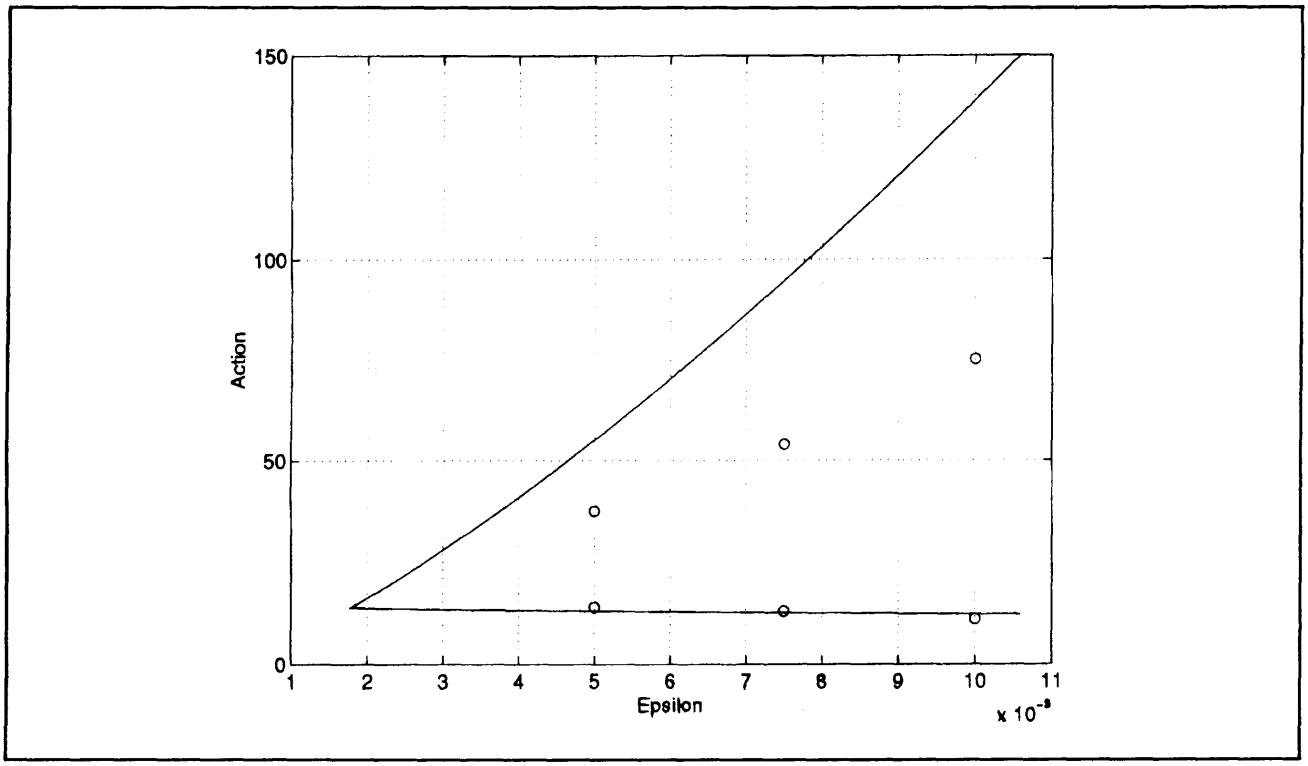

Figure 15. The numerically determined upper and lower bound on the stochastic region in action as the nonlinearity parameter is varied for a frequency ratio of 30.3.

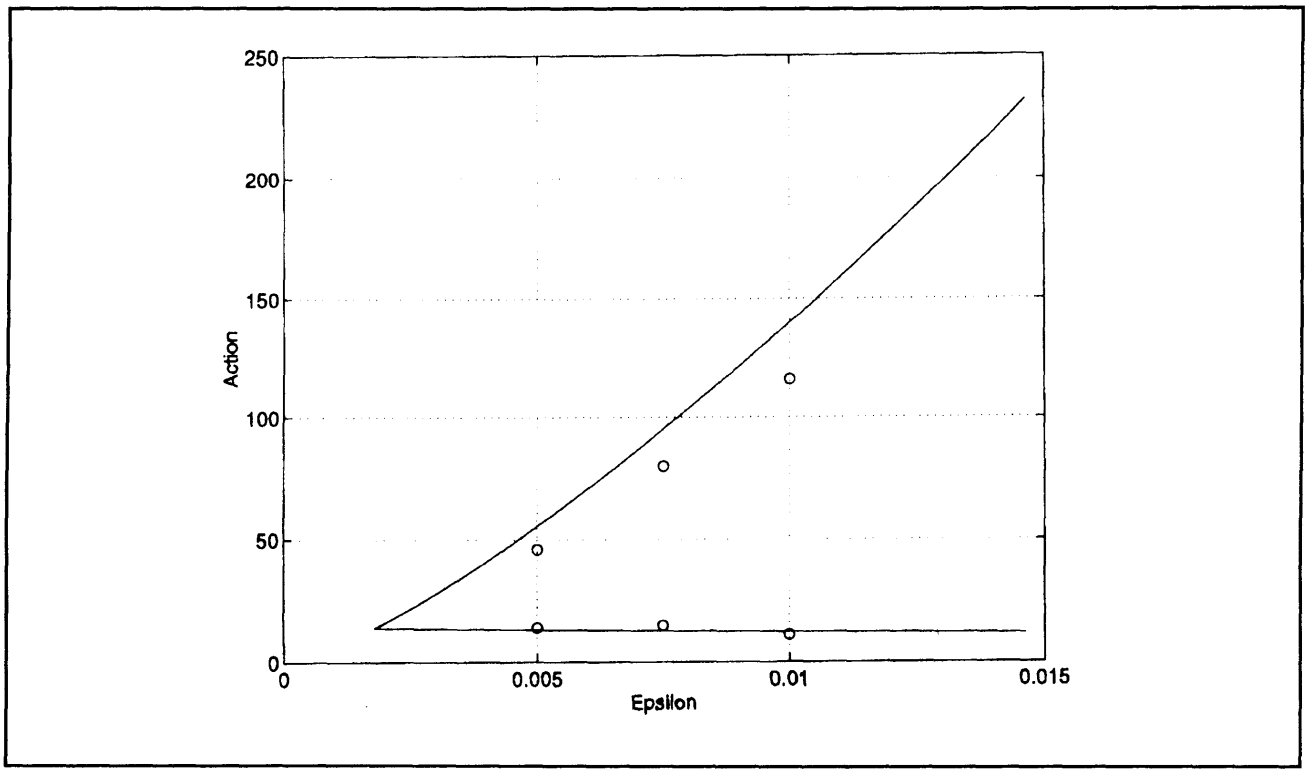

Figure 16. The numerically determined upper and lower bound on the stochastic region in action as the nonlinearity parameter is varied for a frequency ratio of 30.4.

Sagdeev and Zaslavsky[27] have provided some techniques which better motivate the expression derived by Karney for an upper bound and also make it possible to improve its performance as the nearness to resonance varies. In this work, the perturbation is separated into terms that oscillate on a fast time scale and those that oscillate on a slower time scale. The effects of the perturbation on the fast time scale are time averaged because only the averaged effects are seen at the time scale of island formation, and an effective fast potential is created. This potential, which includes some of the nonlinearity of the perturbation, is associated with a new unperturbed system, and a Chirikov condition may be found when this system is perturbed. The upper bound for stochasticity derived using this method is:

$$\varepsilon = \frac{\pi^{1/2} 2^{1/4} |^{3/4}}{\Delta n \bullet T^{9/4}} \qquad (4)$$

where Δn is the number of terms that oscillate on the slower time scale. Notice that since n is the nearest integer to T, by choosing Δn to be 4 and n=T, this method gives a result equivalent to that of Karney (2). Further, the partition of the perturbation into fast and slow terms is somewhat arbitrary. The idea is to identify a group of terms near resonance as the slow terms. The interesting property of this method is that by making the number of terms that are averaged depend on the nearness to resonance of the original system, it appears that Karney's upper bound may be improved. Such work is currently in progress.

1.2.7 Publications

Bers, A., S.D. Schultz, and A.K. Ram. "Mode Conversion to Ion-Bernstein Waves of Fast Alfvén Waves with Finite Poloidal Wavenumber in Tokamak Geometries." *Bull. Am. Phys. Soc.* 40: 1705 (1995).

Fuchs, V., A.K. Ram, S.D. Schultz, A. Bers, and C.N. Lashmore-Davies. "Mode Conversion and Electron Damping of the Fast Alfvén Wave in a Tokamak at the Ion-Ion Hybrid Frequency." *Phys. of Plasmas* 2: 1637 (1995).

Lashmore-Davies, C.N., V. Fuchs, and A.K. Ram. "Strong Electron Dissipation by a Mode Converted Ion Hybrid (Bernstein) Wave." In *Proceedings of the 11th Topical Conference on Radio Frequency Power in Plasmas,* Palm Springs, California, May 17-19, 1995. Eds. R. Prater and V.S. Chan. New York: American Institute of Physics Conference Proceedings 355, 1995, pp. 277-280.

Ram, A.K. "Heating and Current Drive by Mode-Converted Ion-Bernstein Waves." Invited talk, in *Proceedings of the 11th Topical Conference on Radio Frequency Power in Plasmas,* Palm Springs, California, May 17-19, 1995. Eds. R. Prater and V.S. Chan. New York: American Institute of Physics Conference Proceedings 355, 1995, pp. 269-276.

Ram, A.K. "Heating and Current Drive by Mode-Converted Ion-Bernstein Waves." Report PFC/JA-95-18, MIT Plasma Fusion Center, Cambridge, Massachusetts, September 1995.

Ram, A.K., A. Bers, S.D. Schultz, and V. Fuchs. "Interaction of Mode-Converted Ion-Bernstein Waves With Electrons in Tokamaks." In *Proceedings of the International Sherwood Fusion Conference,* Incline Village, Nevada, April 3-5, 1995, Paper 2D17.

Ram, A.K. "Mode-Converted Ion-Bernstein Waves for Heating and Current Drive." *Bull. Am. Phys. Soc.* 40: 1828 (1995).

Ram, A.K., A. Bers, S.D. Schultz, V. Fuchs, A. Bécoulet, and B. Saoutic. "Mode-Converted Ion-Bernstein Waves in Tokamaks." In *Proceedings of the 22nd European Physical Society (EPS) Conference on Controlled Fusion and Plasma Physics,* Bournemouth, England, July 3-7, 1995, Volume 19C, Part IV, pp. 353-356.

Ram, A.K., A. Bers, S.D. Schultz, V. Fuchs, A. Bécoulet, and B. Saoutic. "Mode-Converted Ion-Bernstein Waves in Tokamaks." Report PFC/JA-95-20, MIT Plasma Fusion Center, Cambridge, Massachusetts, September 1995.

Ram, A.K., A. Bers, S.D. Schultz, and V. Fuchs. "RF Wave Effects on the Neoclassical Electron Distribution Function in Tokamaks." In *Proceedings of the International Sherwood Fusion Conference,* Incline Village, Nevada, April 3-5, 1995, Paper 3C17.

---

[27] R.Z. Sagdeev and G.M. Zaslavsky, "Regular and Chaotic Dynamics of Particles in a Magnetic Field," in *Nonlinear Phenomena in Plasma Physics and Hydrodynamics,* ed. R.Z. Sagdeev (Moscow: Mir Publishers, 1986), p. 65.

Saoutic, B., A. Bécoulet, T. Hutter, D. Fraboulet, A.K. Ram, and A. Bers. "Mode Conversion Heating Experiments on Tore Supra." In *Proceedings of the 11th Topical Conference on Radio Frequency Power in Plasmas,* Palm Springs, California, May 17-19, 1995. Eds. R. Prater and V.S. Chan. New York: American Institute of Physics Conference Proceedings 355, 1995, pp. 71-74.

Schultz, S.D., A.K. Ram, and A. Bers. "RF Wave Effects on the Neoclassical Electron Distribution Function in Tokamaks." In *Proceedings of the 11th Topical Conference on Radio Frequency Power in Plasmas,* Palm Springs, California, May 17-19, 1995. Eds. R. Prater and V.S. Chan. New York: American Institute of Physics Conference Proceedings 355, 1995, pp. 263-266.

Schultz, S.D., A.K. Ram, and A. Bers. "RF Wave Effects on the Neoclassical Electron Distribution Function in Tokamaks." Report PFC/JA-95-19, MIT Plasma Fusion Center, Cambridge, Massachusetts, September 1995.

Schultz, S.D., A. Bers, and A.K. Ram. "RF Wave Effects on the Neoclassical Electron Distribution Function in Tokamaks." *Bull. Am. Phys. Soc.* 40: 1703 (1995).

Vacca, L., A. Bers, and A.K. Ram. "RF-Induced Transport of Resonant Minority Species in ICRF-Heated Tokamaks." *Bull. Am. Phys. Soc.* 40: 1706 (1995).

1.3 Physics of Thermonuclear Plasmas

Sponsor

U.S. Department of Energy
Grant DE-FGO2-91ER-54109

Project Staff

Professor Bruno Coppi, Dr. Augusta Airoldi, Dr. Giuseppe Bertin, Dr. Francesca Bombarda, Franco Carpignano, Dr. Giovanna Cenacchi, Marika Contos, William S. Daughton, Dr. Paolo Detragiache, Dr. Matteo Erba, Darin R. Ernst, Gianmarco M. Felice, MöH Kuang, Kevin Lewis, Dr. Riccardo Maggiora, Dr. Stefano Migliuolo, Dr. Francesco Pegoraro, Gregory E. Penn, Evan Reich, Marco Riccitelli, Caterina Riconda, Jeremy Roy, Dr. Suraj Salihu, Dr. Linda E. Sugiyama, George M. Svolos, Dr. Motohiko Tanaka

In this research program, we study the physics of magnetically confined plasmas in regimes relevant to present-day advanced experiments as well as to the planning of new experiments on fusion burning plasmas. The importance of providing an experimental proof of the process of ignition has been underlined[28] by the Panel on Fusion Research of PCAST: "Producing an ignited plasma will be a truly notable achievement for mankind and will capture the public's imagination. Resembling a burning star, the ignited plasma will demonstrate a capability with immense potential to improve human well-being. Ignition is analogous to the first airplane flight or the first vacuum-tube computer."

The Ignitor experiment, proposed by us in 1975, was first suggested and designed on the basis of the known physics of thermonuclear plasmas and present-day technology to reach ignition regimes. Thus, our group has recognized the importance of ignition even when its relevance was not universally acknowledged. ITER, a very large-scale experiment that has been studied more recently as an international undertaking to address the issue of ignition in large-volume, relatively low-density plasmas, has adopted in its design key features that were pioneered by the Ignitor program.

Construction of the Ignitor machine core, with technology based on MIT's Alcator program, is presently underway in Europe.

[28] PCAST, Fusion Review Panel, *PCAST Report* (Washington, D.C.: O.S.T.P., White House, 1995).

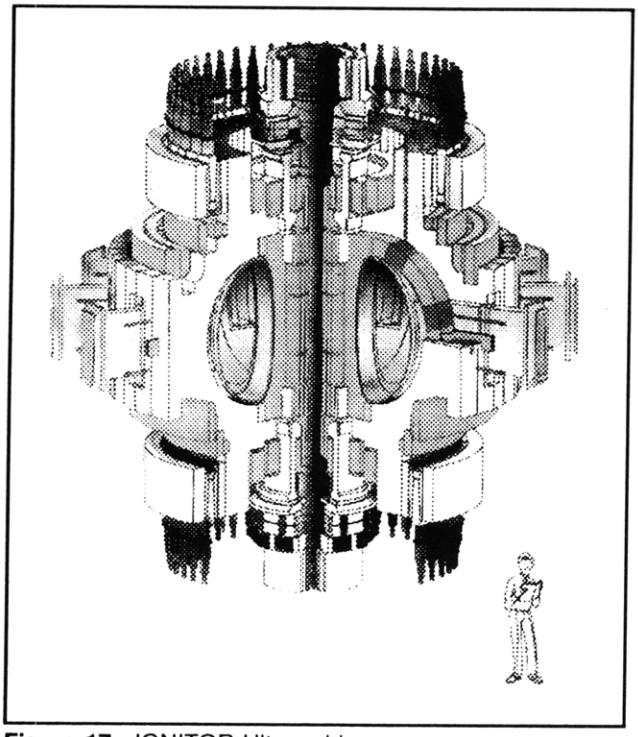

Figure 17. IGNITOR Ult machine.

At MIT, the Alcator C-Mod experiment combines the favorable features of an elongated plasma cross section with a high-magnetic field, to produce high-plasma currents and sustain high-plasma densities. Alcator C-Mod is being successfully operated and is is producing novel results that are of interest to basic plasma physics and to fusion research in general. This machine has characteristics very similar to Megator, which we had studied in the early 1970s in order to produce multimegamperes plasma currents by combining high-magnetic fields, tight aspect ratios and elongated plasma cross sections. Megator was in fact considered a logical evolution of the Alcator program that we had initiated and developed.

There is an increasing body of experimental evidence supporting the elements that characterize the second stability region for finite β plasmas that we had discovered originally, including the good confinement characteristics of regimes with vanishing magnetic shear. Given their intrinsic value, we have followed closely these developments. These regimes can be explored with fusion burning plasmas by experiments of the Ignitor type.

In addition, we have studied Candor, a new machine concept for approaching the fusion burn conditions of tritium-poor plasmas and in particular of D^3 – He mixtures or prevalent-deuterium plasmas (D-D "catalyzed"), where the fraction of fusion energy produced as neutrous is reduced relatively to the commonly considered D-T reactors. In particular, we have devoted considerable attention to the physics of those experiments that employ the high-field, high-current technologies developed for Ignitor and that exploit the favorable properties of the second stability regimes.

At this time, our research program follows two major avenues. First, the basic physical processes of thermonuclear plasmas (equilibrium, stability, transport, etc.) are being studied as they apply to existing or near-term experiments. In this effort, we collaborate with experimentalists and theorists from other research groups both in the United States, e.g., Columbia University, Phillips Laboratory, Princeton University, University of Texas, Lawrence Livermore Laboratory, and abroad, e.g., JET Laboratory, University of Turin, CNR of Milan, etc. This work also involves time-dependent simulations of the plasmas to be produced by the Ignitor-Ult experiment, with particular attention being focused on the evolution of spatial profiles of plasma current and temperature. Collaboration with our colleagues at the laboratories of E.N.E.A. (Italy), as well as in-house code development, plays a major role in this endeavor.

In the following we discuss some salient results of work completed or presently being carried out by members of our research group.

1.3.1 Feasibility of Ignition Experiments: Major Issues for Debate

As indicated earlier, the demonstration of ignition has been repeatedly recognized as the most important objective of fusion research, stressing the principle that "the initial model (experiment) need not resemble the one that is later commercialized; much of what would be learned in a tokamak ignition experiment would be applicable both to more advanced tokamak approaches and to other confinement concepts."[29] For ignition, there are difficult conditions to be met that include the macroscopic stability of the plasma column, the rate of thermal energy transport, the degree of plasma purity, the thermal loading on the first wall, the ability to survive major disruption events, etc. At typical DT ignition parameters, the electron collision frequency exceeds the ω_*-frequencies related to

[29] PCAST Report of the Fusion Review Panel (Washington, D.C.: O.S.T.P., White House, 1995).

the pressure gradients so that the modes producing magnetic reconnection are not of the (relatively benign) collisionless type. For reasons of confinement, the plasma current must be the maximum compatible with the applied toroidal field, corresponding to low values of the safety factor, (e.g., $q_a \simeq 3$), for monotonic shear profiles, or be relatively low (e.g., $q_a \simeq 6$) for a reversed shear configuration. In the case of low q_a, the ideal MHD stability against $m^0 = 1$ and coupled $m^0 = 2$ modes requires that β-poloidal be sufficiently low, such as $\beta_p < 0.3$. Since the central plasma pressure at ignition is prescribed within a rather well defined range, relatively high poloidal fields, B_p, are required. In the case of high q_a, the toroidal field B_T must also be sufficiently high, since there is a limitation on plasma size and on the minimum value of B_p that is acceptable for stability against ballooning modes. In all cases, the required fields are well above those permitted by present superconducting magnet technology.

Thus, the objective of ignition sustained over several (> 10) energy replacement times should be pursued by high-field, normal conducting magnets, and at first by compact experiments igniting at peak densities $n_{e0} \simeq 10^{21}$ m^3 and relatively low temperatures ($T_0 \simeq 12$ keV). Considering the collisional current equilibration time $\tau_I \propto a^2 T^{3/2}$ as another reference for the duration of the ignited state (a is the plasma minor radius), it is clear that relatively small dimensions and low ignition temperatures are compatible with relatively short current pulses. The same argument applies for the density limit, which is commonly related to the average plasma current density and is higher at high fields and compact dimensions.

In the range of high-field machines that have been studied, from Ignitor ($R_0 \simeq 1.32$ m) to Candor ($R_0 \simeq 2.5$ m), the two sets of parameters chosen for construction are based on issues of cost versus benefits. Ignitor is suitable for D-T ignition while Candor is, in principle, capable of reaching D $-^3$He burn conditions. The superconducting ITER device, as presently conceived and assuming that a field of 13 T can be achieved at the coils, does not satisfy macroscopic MHD stability conditions for internal modes, even with flattened pressure profiles when its reference plasma parameters are considered. The smaller "PCAST-machine" that employs normal-conducting magnets (at a cost ~ 6G$) has a similar stability problem when its reference plasma parameters are analyzed.

1.3.2 Physics of Advanced, High-Magnetic Field Experiments

In identifying the optimal performance of an advanced experiment such as Ignitor, presently known constraints on the plasma parameters that can be achieved must be taken into account. These constraints are mutually linked. In particular, Ignitor can operate well within the known limitations for the particle density and the plasma pressure (beta limit). Detailed simulations of the plasma current ramp up and of plasma heating to ignition have been carried out. These are consistent with the engineering constraints of the machine design. A special updated version of the free boundary, 1 + 1/2D JETTO transport code has been employed to study and optimize these characteristics.

The plasma shape and position are controlled to achieve consistency with the reference magnetic confinement configurations, introducing also the first wall contour as a bound. The avoidance of the disruption boundaries in the (l_i, q_ψ) diagram is assured while taking the technical constraints on the poloidal coils (e.g., mechanical and thermal stresses) into account. Transport diffusion coefficients which lead to energy confinement times close to those predicted by "L-mode" scalings have been chosen. Special attention is being given to the influence of the parameters of the outermost region of the plasma column on the evolution of the current density.

1.3.3 Reversed Shear Operation for High-Field Ignition

The improvement of plasma confinement that has been observed during the operation of neutral beam heated tokamaks with nonmonotonic current and q profiles ("reversed shear") introduces the possibility of a new regime of D-T ignition at low density and very low fusion power in high field, magnetically confined plasmas. Reversed shear current profiles should be attainable with modest amounts of auxiliary heating, for discharges running at parameters that are well below the maximum design values that are intended to support full field ohmic or low-auxiliary-power ignition in such machines. In the reversed shear ignition scenario, the current ramp plays an important part in efficient plasma heating to ignition, as well as in establishing the current profile. Reversed shear conditions can be established part way into the initial current ramp-up phase of a discharge. Enhancement of the energy confinement during this part of the ramp provides the optimal heating path to ignition and minimizes the external heating requirement and the fusion power at ignition. The degree of shear

reversal decreases with time after the end of the current ramp, and particularly with the time spent at sub-ignition temperatures. The minimum q falls below two, but can easily be kept well above unity. Machines that can achieve high magnetic fields are likely to gain the greatest benefit from reversed shear ignition. Detailed examples of reversed shear scenarios have been studied for the Ignitor-Ult.[30]

1.3.4 Low-Current Approach to Ignition

The "standard" path to achieve ignition conditions so far has been that of producing plasmas with the maximum current and poloidal field that are compatible with the applied toroidal field and the geometry of the adopted configuration (the low q_a approach.) The other approach that is motivated by recent experiments with reversed shear configuration is with relatively low currents and high fields corresponding to relatively high values of q_a (e.g., $q_a \simeq 6$). While the first approach can be pursued with ohmic heating alone, the second one involves an auxilary heating system that in the case of the Ignitor machine is ICRF. One of the advantages of this approach is that the onset of large scale internal modes can be avoided as $q(\psi)$ is kept above 1 over the entire plasma column. Since quite peaked density profiles are produced in the regimes where enhanced confinement is achieved, the α-particle power level at ignition (and, correspondingly, the thermal load on the first wall) can be reduced relative to the standard, low q_a approach. The possibility of reaching ignition in the reverse shear high q_a regime is considered and that it may be followed by a transition to the low q_a regime, assuring that the excitation of modes involving magnetic reconnection will not undermine the needed degree of confinement. Relevant numerical simulations include the use of the free boundary JETTO code, following the original analysis[31] carried out by the Baldur Code.

1.3.5 Global Stability and Operational Regimes of Ignitor, ITER, and Alcator C-Mod

One of the primary requirements for an experiment capable of approaching ignition conditions is the macroscopic stability of the plasma column. A numerical analysis is carried for two proposed ignition experiments (Ignitor and ITER), concentrating on the stability of their confinement configuration for different plasma pressure and current profiles, using both the PEST and DCON codes (which involve the ideal MHD linearized approximation). Since, in both cases, the aspect ratio is tight (R/a= 2.8 and 2.9, respectively), and the unwinding parameter $q(\psi)$ is less than unity over the inner half of the plasma column, unstable n = 1 modes arise (for which the m = 1,2 poloidal harmonics prevail) and affect a major part of the plasma column ($0 \le r \le 3a/4 \leftrightarrow q(\psi) \le 2$). Here we denote by ψ the normalized poloidal flux variable.

For profiles that are nearly flat up to the q = 1 surface and are represented by $p = p_0(1 - \psi^N)^{3/2}$ with N > 3, pressure driven modes, dominated by the m = 2 harmonic, may be found, depending on the value of $\beta_p = 2\mu_0 < p > /B_p^2$. These modes are unstable for the reference parameters of operation of ITER ($B_T = 5.7T$, $n_0 = 1.5 \times 10^{20}\ m^{-3}$, $T_0 = 20$ keV), but are stable for those of Ignitor ($B_T = 13T$, $n_0 = 0.8 \times 10^{21}\ m^{-3}$, $T_0 = 12$ keV).

For relatively peaked profiles represented[32] by $p = p_0(1 - \psi)^{3/2}$, the numerical analysis produces a stability threshold corresponding to extremely low values of β_p, but the validity of the linearized approximation ($|\tilde{dp}/dr| < |dp/dr|$, $\tilde{p}$ = perturbed plasma pressure) breaks down for very small values of $\tilde{p}$, well before threshold. We consider the predicted instability meaningful when, for instance, $|\tilde{p}|_{BD} \le 0.05p$, where $|\tilde{p}|_{BD}$= value of $|\tilde{p}|$ for breakdown. The value of β_p for the ITER reference discharge leads to values of $|\tilde{p}|_{BD}$ exceeding this threshold while those for Ignitor are well below it.

We have also considered operating conditions corresponding to the reversed shear configuration, with reduced plasma currents ($q(a) \simeq 6$). In this case, stability against ballooning modes become a concern in view of the low values of $\bar{B}_p$ that can be produced (e.g., $\bar{B}_p \simeq 0.5T$ in the case of ITER).

---

[30] B. Coppi, M. Nassi, and L.E. Sugiyama, *Phys. Scripta* 45: 112 (1992).

[31] L.E. Sugiyama, PTP Report 95/03, MIT, 1995.

[32] M. Rosenbluth et al., in *Plasma Physics and Controlled Fusion Research*, IAEA-CN-60/E-P-2 (Vienna: IAEA, 1995).

In order to assess the possibility of the onset of large scale sawtooth oscillations of the plasma column, the excitation of collisional n = 1 modes involving magnetic reconnection is also considered. Thus we have analyzed 12 discharges obtained by Alcator C-Mod[33] with and without RF heating, all exhibiting sawtooth oscillations while ideal MHD stability is verified. Resistive n = 1, m = 1 modes are found to remain unstable according to the theory given in[34] (i.e., the relevant plasma parameters fall in the regions III-IV of the $\lambda_H - \omega_*$ parameter space).

1.3.6 Thermal Transport of Ohmic and ICRF Heated L-mode Plasmas in Alcator C-Mod

The observed similarity in the global thermal confinement between the ohmic and ICRF heated L-mode plasmas opens the possibility that thermal transport in the Alcator C-Mod machine may be described by one transport coefficient for both regimes. A modified form of a transport coefficient previously reported[35] has been used to simulate both ohmic and ICRF discharges over a wide range of parameters. Detailed simulations carried out by means of the BALDUR code reproduce the observed temperature profiles, loop voltage and energy confinement time of the Alcator C-Mod discharges. The coefficient D_e^{th} includes the constraint of profile consistency and is inspired by the properties of the so-called "ubiquitous" mode that can be excited in the presence of a significant fraction of trapped electrons; thus it includes a significant dependence on the electron pressure gradient. The resulting confinement time improves with the plasma current, in agreement with the observations, and contains only a weak dependence on density. In particular, the coefficient is of the form

$$D_e^{th} \propto \left(\omega_{pi} \frac{c^2 \nu_{ee}}{\omega_{pe}^2 V_{the}^2} \right)^{1/3} \frac{I}{enR} \beta_{pe}^* \qquad (1)$$

where $\beta_{pe}^* = (8\pi p_e^{*\prime} < B_\theta^2 >)$ and $p_e^* = a(dp_e/dr)_{max}$. It has been observed from both the experiment and the simulations that β_{pe} is roughly constant for ohmic discharges while it increases with P_H/P_{OH} for ICRF discharges, where P_H is the total heating power. Thus a natural transition between the ohmic and ICRF regimes is included in the coefficient through the pressure gradient dependence. The dependences on the main plasma parameters associated with this diffusion coefficient and the resulting global scalings have been studied and compared with the characteristics of L-mode discharges produced by the machine.

1.3.7 Energy Confinement in High-Field Experiments

In addition to the previously described work on the transport properties of Alcator C-Mod plasmas, which is based on the detailed spatial analysis of a relatively small number of discharges, a more extensive study of global confinement has been undertaken since the beginning of 1995. This also includes a comparison between C-Mod and the FTU machine in Frascati, the only two high-field devices in operation. Their results are especially significant in relation to some assumptions made for Ignitor.[36] The overall dimensions of the two machines are comparable, but they are characterized by some important differences: C-Mod has a D-shaped plasma and a close divertor, FTU is circular and has been operating with a poloidal limiter. Both machines use high-Z materials as plasma facing components.

These machines have been operating in a very similar range of parameters for ohmic plasmas (toroidal field $B_T \sim 5$T, electron density $n_e \sim 10^{20}$ m^{-3}, electron and ion temperature $T_e \leq T_i \sim 1 - 2$ keV), but the energy confinement time seems to exhibit a substantially different behavior. On FTU, which is a circular machine, τ_e follows a neo-Alcator type of scaling, i.e., it increases with density and then saturates, while C-Mod shows a fairly strong positive dependence on the plasma current and a weak, but

---

33 M. Porkolab et al., in *Plasma Physics and Controlled Fusion Research*, IAEA-CN-60/A-1-II-2 (Vienna: IAEA, 1995).

34 B. Coppi et al., in *Plasma Physics and Controlled Fusion Research* (Vienna: IAEA, 1987), vol. 3, p. 397.

35 B. Coppi, et al., in *Proceedings of the 21st EPS Conference on Contributions to Fusion and Plasma Physics,* Montpellier, France, 18B III 520 (1994).

36 F. Bombarda, B. Coppi, W. Daughton, L. Sugiyama, M. Greenwald, A. Hubbard, J. Irby, C. Fiore, J.E. Rice, S. Wolfe, S. Golovato, and Y. Takase, International Sherwood Theory Conference, Incline Village, Nevada, 1995.

negative, dependence on n_e.[37] In ohmic conditions, our analysis shows that on C-Mod, the value of β_p is essentially constant, while on FTU, this is an inverse function of the plasma current. The analysis of some low elongation shots on C-Mod seems to indicate that elongation may be one of the responsible factors for the observed difference. Edge conditions can also effect the global plasma properties, particularly at very low densities, and the scrape-off layer parameters have also been compared. This analysis has confirmed the positive effect of current and elongation on confinement and the high density on plasma purity. Both the FTU and the Alcator C-Mod experiments agree on this for both limiter and divertor configurations, with the additional indication that high-Z first wall materials behave well even at relatively high power loads.

The results on confinement in plasma regimes where ohmic heating is prevalent, as well as at the transition from ohmic heating to injected heating conditions, are of particular interest for the Ignitor program. The results of C-Mod indicate that confinement does not degrade as collisionality decreases at values of β_p close to that for which Ignitor is designed to ignite.

Values of peak electron densities $n_0 \simeq 10^{21}$ m^{-3} have again been obtained with pellet injection, and the successful ICRF heating of high-density plasmas has been demonstrated on C-Mod at power densities about equal to those of the Ignitor design. We have shown[38] that the values of the energy confinement time scaled from those obtained by C-Mod at the lowest collisionality are more than sufficient for ignition.

1.3.8 Recurrent and Random Explosive Events: Relevant Theoretical Models

There are events of relatively brief duration involving, for instance, accelerated or heated particles, excitation of fluctuations, radiation emission that can be related to the onset of different kinds[39] of explosive instabilities and that can recur at regular intervals or randomly. An analytical model[40] is introduced, to represent these events, consisting of a set of nonlinear differential equations which involve a characteristic singularity. This corresponds to an explosive or quasi-explosive event for a "primary" factor (e.g., the population of heated or accelerated particles) or for the relevant plasma fluctuations that are excited when the primary factor exceeds an appropriate threshhold value.

In the case where quasi-explosive events are periodically recurring, a noncanonical Hamiltonian is derived from which the equations for both the primary factor and the excited fluctuation amplitude can be derived. Significant examples of the numerical solution of these equations have been constructed. A comparison is made with the well known Volterra-Lotka equations and with previously considered equations producing sawtooth oscillations of the primary factor.[41] None of these involve singularities and do not describe explosive events.

The random occurrence of this kind of events, involving the primary factor and the fluctuation level, is found by introducing a relatively small time-dependent component of the source of the driving factor or of the instability threshold for the fluctuation level, with a period that is not related to that of the original nonlinear equation. This case has also been illustrated by representative numerical solutions.

1.3.9 Importance of Radial Localization on the Interaction of Fusion Products with High-Frequency Modes

We investigate modes that can interact with high energy reaction products in fusion burning plasmas giving rise to instability for frequencies that correspond to harmonics of the energetic particles' cyclotron frequency. The corresponding modes in a homogeneous plasma would be classified as

---

[37] F. Bombarda, B. Coppi, W. Daughton, L. Sugiyama, C. Fiore, S. Golovato, M. Graf, M. Greenwald, A. Hubbard, J. Irby, B. LaBombard, E. Marmar, M. Porkolab, J.E. Rice, Y. Takase, and S. Wolfe, *Proceedings of the 22nd EPS Conference on Contributions to Fusion and Plasma Physics,* Bournemouth, United Kingdom, 1995; F. Bombarda, B. Coppi, C. Fiore, S. Golovato, M. Greenwald, A. Hubbard, J. Irby, E. Marmar, M. Porkolab, J.E. Rice, Y. Takase, and S. Wolfe, *Bull. Am. Phys. Soc.* 40: 1699 (1995).

[38] P. Detragiache, F. Bombarda, and B. Coppi, *Bull. Am. Phys. Soc.* 40: 1657 (1995).

[39] B. Coppi, M.N. Rosenbluth, and R.N. Sudan, *Ann. Physics* 55: 207 (1969); B. Coppi and A. Friedland, *Astr. J.* 169: 379 (1971).

[40] A.C. Coppi and B. Coppi, *Bull. Am. Phys. Soc.* 40: 1657 (1995).

[41] B. Coppi, A. Taroni, and G. Cenacchi, *Plasma Physics and Controlled Nuclear Fusion* (Vienna: IAEA, 1979), vol. 1, p. 487; L. Chen, R. White, and M.N. Rosenbluth, *Phys. Rev. Lett.* 55: 1122 (1984); B. Basu and B. Coppi, *Phys. Plasmas* 2: 14 (1995).

Magnetosonic-Whistler modes. It is known that in a configuration with inhomogeneous magnetic field, density, and temperature, it is possible to find radially localized solutions,[42] that we call "contained modes," for the perturbed field.

We study new localized solutions for the perturbed fields by solving the equations obtained by linearizing the extended MHD equations, including the Hall term. The main effects associated with this term are to break the symmetry in $\pm k_\perp$, and to include a Whistler-type term in the dispersion equation related to propagation in the direction of the equilibrium magnetic field. In a toroidal shell localized near the edge of the plasma, we find that contained modes exist only for positive values of $K_\perp$. We point out how the existence of this solution is essential that the resonant interaction of the considered modes with relatively few fusion products will yield a positive growth rate.[43]

In fact, traveling modes in the radial direction would convect away the energy gained from the few resonating particles in too short a time to allow a significant increase of their amplitude.

1.3.10 Destabilization of Contained Interacting Modes by Fusion Products

The instability related to the interaction between high-frequency "contained modes" and the fusion products population in a toroidal configuration is being studied.[44] Emphasis is placed on the dependence of the growth rate on finite Larmor radius effects of the fusion products,[45] the characteristics of the particle distribution function,[46] and factors, such as the magnetic drift velocity and bounce-averaging,[47] related to the inhomogeneity of the magnetic field in a toroidal configuration. In particular, we find that a sufficient degree of anisotropy in the energetic particle distribution is required in order to have a positive growth rate for realistic parameters.

Only a small region of phase space is involved in the resonant interactions associated with the considered modes. In the limit where the growth rate is larger than the bounce frequency (local approximation), we find unstable solutions for a class of trapped particles with large perpendicular velocities. Another evaluation of the growth rate γ is obtained in the case, that we consider realistic, where γ is comparable to the average bounce frequency of the interacting particles. We can solve for γ by integrating the linearized Vlasov equation over the unperturbed particle orbits and reducing the integrals through saddle-point approximations.

1.3.11 Nonlinear Saturation of the Parallel Veocity Shear Instability

Plasma flows in the direction parallel to the ambient magnetic field are nearly ubiquitous. They occur naturally in linear plasma columns (e.g., Q-machines) or in toroidal experiments under a variety of conditions. These flows are also observed in the near-Earth environment as solar wind is deflected by the bow shock and flows past the flanks of the magnetosphere. A shear in the flow (i.e., $B \times \nabla V_\parallel \neq 0$) can lead to instabilities and spontaneous break-up of the flow. In driven systems, saturation by quasilinear processes such as relaxation of the velocity gradient is not realistic, thus one is led to consider other processes such as the coupling to a damped mode.

Linear stability analysis predicts two very distinct limits for the velocity shear problem. With relatively large values of the velocity gradient ($dV_\parallel/dx \sim V_{thi}/L_n$), a mode first found by D'Angelo[48] can occur. This mode is characterized by ($\gamma \gg \omega_r$) but is easily stabilized in the presence of significant density gradients. A new dissipative instability can occur for relatively low values of the velocity gra-

---

42 B. Coppi et al., *Phys. Fluids* 29: 4060 (1986).

43 B. Coppi, in *Physics of High Energy Particles in Toroidal Systems,* eds. T. Tajima and M. Okamoto, (New York: AIP Press, 1993).

44 B. Coppi et al., *Phys. Fluids* 29: 4060 (1986); B. Coppi, *Fusion Tech.* 25: 326 (1994).

45 V.S. Belikov and Y.I. Kolesnichenkov, *Fusion Tech.* 25: 258 (1994); Y.P. Chen and S.T. Tsai, *Phys. Plasmas* 2: 3049 (1995).

46 K.G. McClements et al., *Phys. Plasmas* 1: 1918 (1994).

47 Y.P. Chen and S.T. Tsai, *Phys. Plasmas* 2: 3049 (1995); K.G. McClements et al., *Phys. Plasmas* 1: 1918 (1994); N.N. Gorelenkov and C.Z. Cheng, *Phys. Plasmas* 2: 1961 (1995).

48 N. D'Angelo, *Phys. Fluids* 8: 1748 (1965).

dient as first suggested by Coppi.[49] The relevant dissipation can enter through a parallel ion viscosity or ion-neutral collisions. This mode is characterized by ($\omega_r \sim \omega_{*e} \gg \gamma$) and is not stabilized by the presence of density gradients.

In our nonlinear analysis, we consider both the strongly growing D'Angelo mode and Coppi's weakly growing dissipative mode. A plane geometry including both density and velocity gradients is analyzed with two fluid equations. The linear stability of these modes is such that if a mode with wave number $\vec{k}$ is unstable then so are all of its harmonics ($2\vec{k}$, $3\vec{k}$, ...). The inclusion of FLR corrections in the fluid equations introduces a stability boundary in k-space so that we may consider a single linearly unstable eigenmode coupled to a linearly damped harmonic. For Coppi's weakly growing dissipative mode, this scheme results in saturation of the instability at weak to moderate levels, while in the strongly growing D'Angelo limit the scheme breaks down and does not saturate. Both analytical and numerical methods have been used.

1.3.12 Publications

Basu, B., and B. Coppi. *Phys. Plasmas* 2: 14 (1995).

Bombarda, F., B. Coppi, C. Fiore, S. Golovato, M. Greenwald, A. Hubbard, J. Irby, E. Marmar, M. Porkolab, J.E. Rice, Y. Takase, and S. Wolfe. *Bull. Am. Phys. Soc.* 40: 1699 (1995).

Basu, B., and B. Coppi, "Bursting Processes in Plasmas and Relevant Nonlinear Model Equations." *Phys. Plasmas* 2: 1 (1995).

Carpignano, F., B. Coppi, M. Nassi, and the Ignitor Project Group. "The Ignitor Machine: Construction of Prototypes." Interloan report (unpublished).

Coppi, B. "Plasma Transport Barriers: Underlying Processes." Vienna: International Atomic Energy Agency. Forthcoming.

Coppi, B. *Momentum Transport Modes in High Ion Temperature Regimes.* MIT/RLE Report PTP 95/01 1995, *Phys. Lett. A* 201: 66-69 (1995).

Coppi, B. *Presentation to the PCAST Fusion Panel.* MIT/RLE Report PTP 95/02 (1995), presented to the panel in Washington D.C.

Coppi, A.C., and B. Coppi. *Singular Non-linear Equations and Explosive Recurrent Events.* MIT/RLE Report PTP 95/04 (1995).

Detragiache, P., F. Bombarda, and B. Coppi. *Bull. Am. Phys. Soc.* 40: 1657 (1995).

Migliuolo, S. "Isotopic Effect in Transport and the Ubiquitous Mode." *Phys. Lett. A* 198: 341 (1995).

Sugiyama, L.E. *Reversed Shear Ignition in a High Field Toroidal Experiment.* MIT/RLE Report PTP 95/03 (1995).

Zakharov, L., F.M. Levinton, S.H. Batha, R. Budny, M.C. Zarnstorff, S. Migliuolo, and B. Rogers. "Onset and Stabilization of Sawtooth Oscillations in Tokamaks." In *Plasma Physics and Controlled Nuclear Fusion Research 1994* Vienna: I.A.E.A., 1995, paper CN-601 D-III-4.

Abstracts and Conference Presentations

Airoldi, A., G. Cennachi, and B. Coppi. "Enhanced Confinement Conditions and the Ignitor Experiment." 1995 Annual Meeting of th APS, Division of Plasma Physics, Louisville, Kentucky, November 6-10, 1995.

Bombarda, F., B. Coppi, W. Daughton, L. Sugiyama, C. Fiore, S. Golovato, M. Graf, M. Greenwald, A. Hubbard, J. Irby, B. LaBombard, E. Marmar, M. Porkolab, J.E. Rice, Y. Takase, and S. Wolfe. *Proceedings of the 22nd EPS Conference on Contributions to Fusion and Plasma Physics,* Bournemouth, United Kingdom, 1995.

Bombarda, F., B. Coppi, W. Daughton, L. Sugiyama, M. Greenwald, A. Hubbard, J. Irby, C. Fiore, J.E. Rice, S. Wolfe, S. Golovato, and Y. Takase. International Sherwood Theory Conference, Incline Village, Nevada, 1995.

Bombarda, F., B. Coppi, C. Fiore, S. Golovato, M. Greenwald, A, Hubbard, J. Irby, E. Marmar, M. Porkolab, J.E. Rice, Y. Takase, and S. Wolfe. "Transport Regimes in High Density Plasmas Produced by Alcator C-Mod." 1995 Annual

[49] B. Coppi, MIT Report *Plasma Phys. Contr. Fusion* 36: B107 (1994); J.M. Finn, *Phys. Plasmas* 2: 4400 (1995).

Meeting of th APS, Division of Plasma Physics, Louisville, Kentucky, November 6-10, 1995.

Bombarda, F., B. Coppi, W. Daughton, L. Sugiyama, M. Greenwald, A. Hubbard, J. Irby, C. Fiore, J. Rice, S. Wolfe, and B. LaBombard, "The Ignitor Experiment and Relevance of the Alcator C-Mod Confinement Results." International Sherwood Fusion Theory Conference, Incline Village, Nevada, April 3-5, 1995.

Bonoli, P.T., M. Porkolab, L. Sugiyama, and C. Kessel. "Simulations of MHD Stable Operating Scenarios in the Tokamak Physics Experiment (TPX)." 1995 Annual Meeting of th APS, Division of Plasma Physics, Louisville, Kentucky, November 6-10, 1995.

Carpignano, F., B. Coppi, M. Nassi, and the Ignitor Project Group. "Prototypes Construction in the Ignitor Program." 1995 Annual Meeting of th APS, Division of Plasma Physics, Louisville, Kentucky, November 6-10, 1995.

Cennachi, G., B. Coppi, F. Ferro, M. Gasparotto, C. Rita, M. Roccella, and L. Lanzavecchia. "Plasma Evolution Scenarios in the Ignitor-Ult Experiment." 1995 Annual Meeting of th APS, Division of Plasma Physics, Louisville, Kentucky, November 6-10, 1995.

Coppi, A.C., and B. Coppi. "'Explosive' Periodic Bursts and Generalized Bursting Equation." 1995 Annual Meeting of th APS, Division of Plasma Physics, Louisville, Kentucky, November 6-10, 1995.

Coppi, B., and L.E. Sugiyama. "Collisionless Magnetic Reconnection." 1995 Annual Meeting of th APS, Division of Plasma Physics, Louisville, Kentucky, November 6-10, 1995.

Coppi, B., P. Detragiache, and S. Migliuolo. "The Issue of Internal Modes in Ignition Experiments." 1995 Annual Meeting of th APS, Division of Plasma Physics, Louisville, Kentucky, November 6-10, 1995.

Coppi, B., and L.E. Sugiyama. "Collisionless Magnetic Reconnection in Well-Confined Plasmas." International Sherwood Fusion Theory Conference, Incline Village, Nevada, April 3-5, 1995.

Coppi, B., P. Detragiache, and S. Migliuolo. "The Issue of Internal Modes in Ignition Experiments." International Sherwood Fusion Theory Conference, Incline Village, Nevada, April 3-5, 1995.

Daughton, W., and B. Coppi. "Anamolous Transport of Angular Momentum and Microscopic Dissipative Processes." 1995 Annual Meeting of th APS, Division of Plasma Physics, Louisville, Kentucky, November 6-10, 1995

Daughton, W., B. Coppi, L.E. Sugiyama, M. Greenwald, F. Bombarda, and Y. Takase. "Transport Simulations of the Alcator C-Mod Plasmas." International Sherwood Fusion Theory Conference, Incline Village, Nevada, April 3-5, 1995.

Detragiache, P., F. Bombarda, and B. Coppi. "Recent Results on Confinement: Physics Basis of Ignitor." 1995 Annual Meeting of th APS, Division of Plasma Physics, Louisville, Kentucky, November 6-10, 1995.

Ernst, D.R., B. Coppi, S.D. Scott, and The TFTR Group. "Transport Analysis of Rotating TFTR Plasmas and Modes Driven by Velocity Gradients." 1995 Annual Meeting of th APS, Division of Plasma Physics, Louisville, Kentucky, November 6-10, 1995.

Gatto, R., D. Hua, and S. Migliuolo. "Analytical and Numerical Solutions of the Tearing Modes Linear Stability Equation." International Sherwood Fusion Theory Conference, Incline Village, Nevada, April 3-5, 1995.

Lanzavecchia, L., B. Coppi, R. Andreani, M. Gasporotto, C. Rita, M. Roccella, G. Dalmut, R. Marabotto, G. Galasso, and I. Montanari. "Poloidal Field Coils Design for the Ignitor-Ult Experiment." 1995 Annual Meeting of th APS, Division of Plasma Physics, Louisville, Kentucky, November 6-10, 1995.

Migliuolo, S. "Nonlinear and Nonlocal Dynamics of the Equatorial Spread-F." 1995 Annual Meeting of th APS, Division of Plasma Physics, Louisville, Kentucky, November 6-10, 1995.

Migliuolo, S., J.P. Friedberg, J. Kesner, and J.J. Ramos. "Ideal MHD Analysis of TFTR Discharges." International Sherwood Fusion Theory Conference, Incline Village, Nevada, April 3-5, 1995.

Park, W., G.Y. Fu, H.R. Strauss, and L. Sugiyama. "Multi-Level Numerical Simulation of Tokamak Plasmas." 1995 Annual Meeting of th APS, Division of Plasma Physics, Louisville, Kentucky, November 6-10, 1995.

Penn, G., B. Coppi, and W. Daughton. "Transport Barrier in Very High Temperature Plasmas."

International Sherwood Fusion Theory Conference, Incline Village, Nevada, April 3-5, 1995.

Penn, G., and B. Coppi, "The Interaction of High Energy Particles with Modes near Harmonics of the Cyclotron Frequency." C. Riconda, 1995 Annual Meeting of th APS, Division of Plasma Physics, Louisville, Kentucky, November 6-10, 1995.

Penn, G., C. Riconda, and B. Coppi. "The Distribution of Fusion Products in a Tokamak Reactor, and Related Effects." 1995 Annual Meeting of th APS, Division of Plasma Physics, Louisville, Kentucky, November 6-10, 1995.

Porkolab, M., P.T. Bonoli, S. Golovato, J. Ramos, L. Sugiyama, Y. Takase, C. Kessel, and W. Nevins. "Advanced Tokamak Physics Scenarios in Alcator C-Mod." 1995 Annual Meeting of th APS, Division of Plasma Physics, Louisville, Kentucky, November 6-10, 1995.

Pravia, M., B. Coppi, W. Daughton, L. Sugiyama, F. Bombarda. M. Greenwald, and The Alcator C-Mod Team. "Transport Simulations of Alcator-C-Mod ICRF Plasmas." Annual Meeting of the APS, Division of Plasma Physics, Louisville, Kentucky, November 6-10, 1995.

Qu, Y.L., J.E. Rice, E.S. Marmar, and F. Bombarda. "X-Ray Observations of Toroidal Rotation in Alcator C-Mod Plasmas." 1995 Annual Meeting of th APS, Division of Plasma Physics, Louisville, Kentucky, November 6-10, 1995.

Rice, J.E., J.L. Terry, E.S. Marmar, and F. Bombarda. "X-Ray Observations of Up-Down Impurity Density Asymmetries in Alcator C-Mod Plasmas." 1995 Annual Meeting of th APS, Division of Plasma Physics, Louisville, Kentucky, November 6-10, 1995.

Riconda, C., B. Coppi, and G. Penn. "Emission Above the Ion Cyclotron Frequency in a Nonhomogeneous Magnetic Field." International Sherwood Fusion Theory Conference, Incline Village, Nevada, April 3-5, 1995.

Sugiyama, L.E., and W. Park. "Two Fluid Studies of Low m, n Instabilities." 1995 Annual Meeting of th APS, Division of Plasma Physics, Louisville, Kentucky, November 6-10, 1995.

Sugiyama, L.E. "Two Fluid Studies of Tokamak Plasmas." MHD Workshop on the Beta Limit in Long Pulse Discharges, La Jolla, CA, September 11-14, 1995.

Sugiyama, L.E. "Reversed Shear Considerations for Ignition Experiments." MHD Workshop on the Effects of Reversed Shear on the Beta Limit, Princeton, New Jersey, December 14-15, 1995.

Sugiyama, L.E., and W. Park. "The Two Fluid Model and Stabilization of the m = 1, n = 1 Mode in a Tokamak." International Sherwood Fusion Theory Conference, Incline Village, Nevada, April 3-5, 1995.

Tajima, T., and B. Coppi. "Considerations on Plasma Transport Barriers." International Sherwood Fusion Theory Conference, Incline Village, Nevada, April 3-5, 1995.

Wang, Y., J. Rice, F. Bombarda, G. McCracken, E. Marmar, R. Granetz, J. Terry, B. Labombard, and M. Graf. "Impurity screening study of various Alcator C-Mod Plasmas." 1995 Annual Meeting of th APS, Division of Plasma Physics, Louisville, Kentucky, November 6-10, 1995.